

Preserving Task-Relevant Information Under Linear Concept Removal

Floris Holsteg^{*†‡} Shauli Ravfogel^{*◇} Bram Wouters[†]

University of Amsterdam, Department of Quantitative Economics[†]

New York University, Center for Data Science[◇]

Tinbergen Institute[‡]

Abstract

Modern neural networks often encode unwanted concepts alongside task-relevant information, leading to fairness and interpretability concerns. Existing post-hoc approaches can remove undesired concepts but often degrade useful signals. We introduce SPLICE—Simultaneous Projection for LInear concept removal and Co-variance prEservation—which eliminates sensitive concepts from representations while exactly preserving their covariance with a target label. SPLICE achieves this via an oblique projection that “splices out” the unwanted direction yet protects important label correlations. Theoretically, it is the unique solution that removes linear concept predictability and maintains target covariance with minimal embedding distortion. Empirically, SPLICE outperforms baselines on benchmarks such as Bias in Bios and Winobias, removing protected attributes while minimally damaging main-task information.

1 Introduction

Deep neural networks (DNNs), including Language Models (LMs), have achieved great success in natural language processing (NLP) by learning rich representations of text, often referred to as embeddings [Cao, 2024, Wang et al., 2024a]. These embeddings were shown to also encode undesired information, such as markers of gender, leading to biased predictions [Bolukbasi et al., 2016]. In response, a variety of concept-removal methods has been developed to remove undesired information from embeddings. Examples of such methods are iterative nullspace projection (INLP, Ravfogel et al. [2020]), Linear adversarial concept erasure (RLACE, Ravfogel et al. [2022]), Spectral Attribute Removal (SAL, Shao et al. [2023]), and Least-squares Concept Erasure (LEACE, Belrose et al. [2023]). The shared objective of these methods is to make a concept—such as gender—undetectable by any linear classifier, while preserving the original embeddings as much as possible.

Previous work has noted that a drawback of post-hoc concept-removal methods is that in addition to removing a particular concept, they tend to also eliminate other concepts and information from embeddings [Feder et al., 2021, Belinkov, 2022, Kumar et al., 2022, Guerner et al., 2025, Ravfogel et al., 2025]. Consider, for instance, a scenario where we wish to remove the effect of gender markers on a classifier that screens CVs for job applications. Naively applying concept-erasure techniques to removes gender markers from the input representations may inadvertently harm the model’s performance on the primary task of profession prediction, since in real-world data, certain professions are strongly associated with gender. As a result, the erasure may distort relevant information, undermining both interpretability and utility.

In this paper, we seek to address a key drawback of post-hoc concept-removal methods. Our contribution is to introduce SPLICE, a projection that (similar to LEACE or SAL) prevents any

^{*}Equal contribution. Correspondence to f.g.holsteg@uva.nl

linear classifier from predicting a concept, while also preserving the covariance with a task of interest. Mathematically, we construct an oblique projection that places the covariance between the representations and a protected attribute in its *kernel*, while maintaining the covariance between the representations and the main-task label in its *range*.

We prove that if a linear classifier is re-fitted after projection without regularization, *any* two projections that share the same kernel (i.e., that linearly erase the same subspace) will induce identical loss. In that sense, SPLICE and previous methods such as LEACE [Belrose et al., 2023] (as well as more naive versions that do not explicitly aim to maintain the *minimality* of the projection) are all equivalent. For causal model interventions aiming to interpret its behavior—a situation where the underlying model is necessarily frozen—we argue that SPLICE may perform a more surgical intervention, akin to minimizing the side effects of erasure on related concepts (e.g., removing *gender bias* while preserving *grammatical gender*). Empirically, we show that in a realistic classification setting, SPLICE improves fairness in a highly challenging, imbalanced scenario, and removes stereotypes while maintaining correlated factual information.

2 Related work

Concept-removal: in response to growing concerns about DNNs relying on problematic or harmful concepts, a range of adversarial methods were developed to remove concepts from the embeddings of neural networks [Xie et al., 2017, Zhang et al., 2018]. However, these methods were later deemed unsuccessful at removing concepts [Elazar and Goldberg, 2018]. Subsequently, many works (including this) focused on preventing a linear classifier from predicting a concept as a more tractable alternative. This line of work is supported by the *linear subspace hypothesis* [Bolukbasi et al., 2016], which argues that concepts are represented in linear subspaces of embeddings (for a more elaborate discussion, see Park et al. [2024]).

Existing linear concept-removal methods: iterative nullspace projection (INLP, Ravfogel et al. [2020]) trains a linear classifier to predict a concept, and projects embeddings to the nullspace of the parameters of the linear classifier. This is repeated until the concept can no longer be predicted by the linear classifier. Relaxed Linear Adversarial Concept Erasure (RLACE, Ravfogel et al. [2022]) trains an orthogonal projection matrix such that a concept cannot be predicted by a linear classifier. These works were followed up by Least-squares Concept Erasure (LEACE, Belrose et al. [2023]), which ensures that no linear classifier can predict the concept (hereafter referred to as *linear guardedness*) while minimally altering the embeddings. Spectral attribute removal (SAL, Shao et al. [2023]) projects the embeddings orthogonal to the first k eigenvectors of the covariance matrix $\text{Cov}(\mathbf{x}, \mathbf{z})$. Mean Projection (MP, [Haghighatkah et al., 2022]) projects embeddings to the nullspace of the mean difference between embeddings with and without concepts. It is equivalent to SAL when the concept is binary. SAL and MP also guarantee linear guardedness.

Linear concept-removal while preserving task-relevant information: previous work suggests that linear concept-removal methods remove task-relevant information in addition to the concept they seek to remove [Belinkov, 2022, Kumar et al., 2022, Guerner et al., 2025]. In response, several alternatives have been proposed to address this issue, all removing a different linear subspace [Dev et al., 2021, Holstege et al., 2024, Bareeva et al., 2024, Shi et al., 2024]. However, each of these approaches sacrifices linear guardedness in order to retain more task relevant information. An alternative approach is to explicitly optimize for fairness while maintaining task performance [Shen et al., 2021]. However, this approach is more resource-intensive, as it cannot be applied to the frozen representations of a pretrained model. Moreover, because it modifies the original representations, it is unsuitable for scenarios where the intervention is intended to simulate causal experiments on the behavior of a pretrained LM, as discussed in section 4.2.

In this paper, we study how to retain task-relevant information while maintaining linear guardedness. Recent work has also focused on applying projections to parameters of DNNs instead of embeddings [Limisiewicz et al., 2024, 2025, Arditi et al., 2024]. This is outside of the scope of this paper.

3 Theory

We consider random vectors $\mathbf{x} \in \mathbb{R}^d$ and $\mathbf{z} \in \mathcal{Z}$. Here, \mathbf{x} can be any vector of features, but should generally be thought of as embeddings of a deep neural network. In most cases we consider, they are

the last-layer embeddings. The vector \mathbf{z} represents the concept to be removed. It can be a binary or one-hot-encoded label, or continuous in the case of a regression setting.

The general idea of linear concept removal is to apply an affine transformation $r(\mathbf{x}) = \mathbf{P}\mathbf{x} + \mathbf{b}$, where $\mathbf{P} \in \mathbb{R}^{d \times d}$ and $\mathbf{b} \in \mathbb{R}^d$, that prevents classifiers from recovering the concept represented by \mathbf{z} from the features \mathbf{x} . A special case of this objective aims to achieve *linear guardedness* [Ravfogel et al., 2023, Belrose et al., 2023], the inability of *linear* classifiers to predict the concept. Concretely, they show that linear guardedness is equivalent to zero covariance between the transformed features and the concept to be removed, i.e., $\text{Cov}(r(\mathbf{x}), \mathbf{z}) = \mathbf{P}\Sigma_{\mathbf{x},\mathbf{z}} = \mathbf{0}$, where $\Sigma_{\mathbf{x},\mathbf{z}} = \text{Cov}(\mathbf{x}, \mathbf{z})$ is the cross-covariance matrix of \mathbf{x} and \mathbf{z} , and the symbol $\mathbf{0}$ can refer both to a zero vector and zero matrix. This condition, to which we will refer as the *kernel constraint*, only requires the kernel of \mathbf{P} to contain the column space $\text{colsp}(\Sigma_{\mathbf{x},\mathbf{z}}) \subseteq \mathbb{R}^d$. The intuition is that \mathbf{P} removes directions in the feature space that are linearly correlated with \mathbf{z} , making it impossible for linear classifiers to use the transformed features to predict \mathbf{z} . Importantly, this means that the requirement of linear guardedness does not uniquely determine the affine transformation. Belrose et al. [2023] use this freedom to minimize the impact of the transformation on the distance between the original and projected representations, driven by the intuition that the minimal-norm projection would minimally damage *other* semantic information encoded therein.

This problem turns out to have a closed-form solution: Belrose et al. [2023] show that for centered data, i.e., $\mathbb{E}[\mathbf{x}] = \mathbf{0}$, the constrained optimization problem

$$\arg \min_{\mathbf{P} \in \mathbb{R}^{d \times d}} \mathbb{E} \left[\|\mathbf{P}\mathbf{x} - \mathbf{x}\|_{\mathbf{M}}^2 \right], \quad \mathbf{P}\Sigma_{\mathbf{x},\mathbf{z}} = \mathbf{0} \quad (1)$$

has solution $\mathbf{P}_{\text{LEACE}}^* = \mathbf{W}^+ \mathbf{U} \mathbf{U}^T \mathbf{W}$, where $\mathbf{W} = (\Sigma_{\mathbf{x},\mathbf{x}}^{1/2})^+$ is a whitening matrix and \mathbf{U} is a matrix whose orthonormal columns span the orthogonal complement of $\text{colsp}(\mathbf{W}\Sigma_{\mathbf{x},\mathbf{z}})$, which is the column space of the covariance matrix between \mathbf{x} and \mathbf{z} after whitening. Here, we denote by $\Sigma_{\mathbf{x},\mathbf{x}} \in \mathbb{R}^{d \times d}$ the variance-covariance matrix of \mathbf{x} , by \mathbf{A}^+ the Moore-Penrose pseudoinverse of a matrix \mathbf{A} , and by $\mathbf{A}^{1/2}$ the p.s.d. square root of a p.s.d. matrix \mathbf{A} . The resulting transformation is an oblique projection with kernel $\text{colsp}(\Sigma_{\mathbf{x},\mathbf{z}})$ and range determined by the whitening matrix \mathbf{W} . The intuition is that this is the smallest possible kernel that satisfies the kernel constraint in equation 1, while the chosen range minimizes the distortion caused by a projection with this kernel.

3.1 SPLICE: Ensuring linear guardedness while preserving task-relevant covariance

The LEACE projection ensures linear guardedness while minimizing the distortion of the features, but is oblivious of the main task of the model. A small expected norm squared may not optimally preserve information that is actually useful for the task at hand. Suppose now there is a random vector $\mathbf{y} \in \mathcal{Y}$ that represents task-relevant information. Similar to the concept vector \mathbf{z} , it can be binary, one-hot encoded or continuous. We conjecture that task-relevant information in the features \mathbf{x} is located in the directions that linearly covariate with \mathbf{y} . In other words, it is located in the column space of the covariance matrix $\Sigma_{\mathbf{x},\mathbf{y}} = \text{Cov}(\mathbf{x}, \mathbf{y})$; indeed, *removing* this particular subspace completely prevents linear classification [Belrose et al., 2023].

In order to preserve this task-relevant information, we require the affine transformation $r(\mathbf{x}) = \mathbf{P}\mathbf{x} + \mathbf{b}$ not only to produce features that are linearly guarded for \mathbf{z} , but also to leave the covariance between \mathbf{x} and \mathbf{y} invariant. For this approach we cast the name SPLICE (Simultaneous Projection for Linear concept removal and Covariance prEservation), which can be seen as an extension of LEACE. It eliminates sensitive concepts from representations while exactly preserving their covariance with a target label. The SPLICE optimization problem is formulated in Theorem 1 and its solution is given by equation 4, which is the main theoretical contribution of this paper.

Theorem 1. *Let \mathbf{x} and \mathbf{z}, \mathbf{y} be random vectors with finite second moments, non-zero covariances between \mathbf{x} and \mathbf{z} , and between \mathbf{x} and \mathbf{y} , and $\mathbb{E}[\mathbf{x}] = \mathbf{0}$. Let $\mathbf{W} = (\Sigma_{\mathbf{x},\mathbf{x}}^{1/2})^+$ be a whitening matrix. Define linear subspaces $\mathcal{U}^\perp = \text{colsp}(\mathbf{W}\Sigma_{\mathbf{x},\mathbf{z}})$ and $\mathcal{V} = \text{colsp}(\mathbf{W}\Sigma_{\mathbf{x},\mathbf{y}}) + \mathcal{U}^-$, where $\mathcal{U}^- = \mathcal{U} \cap (\text{colsp}(\mathbf{W}\Sigma_{\mathbf{x},\mathbf{z}}) + \text{colsp}(\mathbf{W}\Sigma_{\mathbf{x},\mathbf{y}}))^\perp$. Assume $\mathcal{U}^\perp \cap \text{colsp}(\mathbf{W}\Sigma_{\mathbf{x},\mathbf{y}}) = \{\mathbf{0}\}$. Then the optimization problem*

$$\arg \min_{\mathbf{P} \in \mathbb{R}^{d \times d}} \mathbb{E} \left[\|\mathbf{P}\mathbf{x} - \mathbf{x}\|_{\mathbf{M}}^2 \right] \quad (2)$$

subject to the two constraints

$$\mathbf{P}\Sigma_{\mathbf{x},\mathbf{z}} = \mathbf{0}, \quad \text{and} \quad \mathbf{P}\Sigma_{\mathbf{x},\mathbf{y}} = \Sigma_{\mathbf{x},\mathbf{y}}, \quad (3)$$

to be referred to as the kernel and range constraint, respectively, has the solution

$$\mathbf{P}_{\text{SPLICE}}^* = \mathbf{W}^+ \mathbf{V} (\mathbf{U}^T \mathbf{V})^{-1} \mathbf{U}^T \mathbf{W}, \quad (4)$$

where \mathbf{U} and \mathbf{V} are matrices whose orthonormal columns span \mathcal{U} and \mathcal{V} , respectively.

The proof of Theorem 1 is given in Appendix A.1. Compared to the LEACE optimization problem, the only difference is the additional condition of preserving task-relevant information, $\mathbf{P}\Sigma_{\mathbf{x},\mathbf{y}} = \Sigma_{\mathbf{x},\mathbf{y}}$, which we refer to as the *range constraint*. Similar to LEACE, $\mathbf{P}_{\text{SPLICE}}^*$ is an oblique transformation with kernel $\text{colsp}(\Sigma_{\mathbf{x},\mathbf{z}})$. The difference lies in the range, which now contains $\text{colsp}(\Sigma_{\mathbf{x},\mathbf{y}})$ in order to fulfill the range constraint. Intuitively, the freedom that the LEACE optimization problem gives to the choice of the range is partially used to preserve the task-relevant information, i.e., the covariance between \mathbf{x} and \mathbf{y} . The remainder of the freedom is used to minimize the distortion caused by the affine transformation, leading to whitening and unwhitening, similar to LEACE.

We note that, perhaps counter-intuitively, SPLICE is not necessarily equivalent to LEACE if $\text{colsp}(\Sigma_{\mathbf{x},\mathbf{z}})$ and $\text{colsp}(\Sigma_{\mathbf{x},\mathbf{y}})$ are orthogonal subspaces. Only if those subspaces are orthogonal *after* whitening, SPLICE and LEACE are equivalent. In that case the orthogonal projection of LEACE then already contains the task-relevant directions $\text{colsp}(\mathbf{W}\Sigma_{\mathbf{x},\mathbf{y}})$ in its range. We also note that, similar to LEACE [Belrose et al., 2023], in the case of non-centered data, i.e., $\mathbb{E}[\mathbf{x}] \neq \mathbf{0}$, the optimal affine transformation requires the addition of a constant $\mathbf{b}_{\text{SPLICE}}^* = \mathbb{E}[\mathbf{x}] - \mathbf{P}_{\text{SPLICE}}^* \mathbb{E}[\mathbf{x}]$. Finally, in Figure 1 we give a visual illustration of the steps of the projection matrix suggested by Theorem 1.

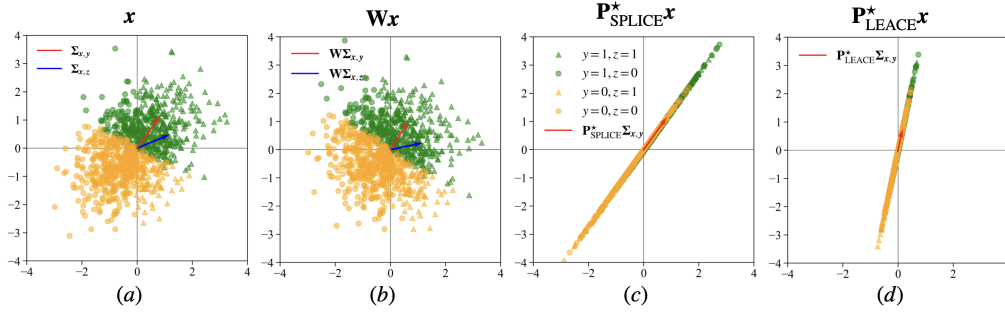


Figure 1: Illustration of the different steps for the projection suggested by Theorem 1 on two-dimensional data. The data (a) is whitened (b). Then, we use $\mathbf{V}(\mathbf{U}^T \mathbf{V})^{-1} \mathbf{U}^T$ to project parallel to $\mathbf{W}\Sigma_{\mathbf{x},\mathbf{z}}$ onto $\mathbf{W}\Sigma_{\mathbf{x},\mathbf{y}}$, and subsequently unwhiten (c). With LEACE, the $\Sigma_{\mathbf{x},\mathbf{y}}$ is altered (d).

3.2 Last-layer linear concept removal with re-training

The first use case of SPLICE we consider is linear concept removal applied to the embeddings of a DNN, after which a linear classifier is fitted on the transformed embeddings. This can be useful if it is demanded that a predictive model does not make use of sensitive concepts, like gender or race.

If we compare SPLICE with other concept removal methods that guarantee linear guardedness, namely LEACE and SAL [Shao et al., 2023], we observe that they are all projections with the same kernel $\text{colsp}(\Sigma_{\mathbf{x},\mathbf{z}})$. They differ in the choice of the range. Interestingly, we find that the predictions of a linear classifier that is trained without regularization on the transformed embeddings are not affected by this choice of the range. In other words, all concept removal methods that ensure linear guardedness will lead to the same predictions after re-training a linear classifier without regularization. We verify this empirically in Appendix B.1.

This result is formalized in Theorem 2, in which we consider training a model $f(\mathbf{x}; \boldsymbol{\theta})$ that only depends on the embeddings \mathbf{x} and parameters $\boldsymbol{\theta}$ through their inner product. Examples of such models are linear and logistic regression, the latter typically being used as the linear classifier re-trained on the embeddings. Before fitting, an projection is applied to the embeddings. We consider two projections that have the same kernel, but different ranges. Theorem 2 shows that, in the case of a strictly convex loss function without regularization, both fitted models lead to the same predictions.

Theorem 2 (Equivalent predictions after oblique re-training). *Consider observations $(\mathbf{x}, \mathbf{y}) \in \mathbb{R}^d \times \mathcal{Y}$ and a model $f(\mathbf{x}; \boldsymbol{\theta})$ that only depends on the inputs \mathbf{x} and parameters $\boldsymbol{\theta}$ through their inner product,*

i.e., $f(\mathbf{x}; \boldsymbol{\theta}) = f(\mathbf{x}^\top \boldsymbol{\theta})$. Suppose we have data $\{(\mathbf{x}_k, \mathbf{y}_k)\}_{k=1}^n$, which is organized in a design matrix $\mathbf{X} \in \mathbb{R}^{n \times d}$ and $\mathbf{Y} \in \mathbb{Y}^n$. Before fitting the model, we apply an oblique transformation to the features \mathbf{x} . We consider two projections that have the same kernel $\mathcal{U} \in \mathbb{R}^d$, but different ranges $\mathcal{A}, \mathcal{B} \in \mathbb{R}^d$. We denote the corresponding transformation matrices as $\mathbf{P}_\mathcal{A}, \mathbf{P}_\mathcal{B}$, and we define $\mathbf{x}_\mathcal{A} = \mathbf{P}_\mathcal{A} \mathbf{x} \in \mathcal{A}$ and $\mathbf{x}_\mathcal{B} = \mathbf{P}_\mathcal{B} \mathbf{x} \in \mathcal{B}$. Let $\mathcal{L}(\mathbf{X}\boldsymbol{\theta}, \mathbf{Y})$ be a loss function with a unique minimizer. Then the following two minimizers

$$\boldsymbol{\theta}_\mathcal{A}^* = \arg \min_{\boldsymbol{\theta} \in \mathcal{A}} \mathcal{L}(\mathbf{X}_\mathcal{A} \boldsymbol{\theta}, \mathbf{Y}), \quad \boldsymbol{\theta}_\mathcal{B}^* = \arg \min_{\boldsymbol{\theta} \in \mathcal{B}} \mathcal{L}(\mathbf{X}_\mathcal{B} \boldsymbol{\theta}, \mathbf{Y}) \quad (5)$$

lead to the exact same predictions. In other words, $\mathbf{x}_\mathcal{A}^\top \boldsymbol{\theta}_\mathcal{A}^* = \mathbf{x}_\mathcal{B}^\top \boldsymbol{\theta}_\mathcal{B}^*$ for any $\mathbf{x} \in \mathbb{R}^d$.

The proof of Theorem 2 is given in Appendix A.2. The intuition behind this result is that there exists an invertible linear transformation between the data after $\mathbf{P}_\mathcal{A}$ and the data after $\mathbf{P}_\mathcal{B}$. In other words, the choice of the range does not determine how much (linear) information about the target variable is lost in the oblique projection. This is solely determined by the choice of the kernel.

We point out that the assumption of unique minimizers corresponds to strictly convex loss functions, which is a common assumption for linear and logistic regression [Albert and Anderson, 1984]. In addition, note that the constraints in equation 5 of the parameters to \mathcal{A}, \mathcal{B} is without loss of generality. Because of the inner product, components perpendicular to the subspaces do not affect predictions.

3.3 When does changing the range matter?

Theorem 2 provides a case where SPLICE will lead to the same predictions as other concept removal methods that ensure linear guardedness (e.g., SAL and LEACE). Here, we identify two practical cases where applying projections with the same kernel and different ranges will typically lead to different predictions.

1. **When re-training the last layer with regularization:** if we include a regularization term (such as $\|\boldsymbol{\theta}\|_2$ or $\|\boldsymbol{\theta}\|_1$) in our loss function \mathcal{L} , then it no longer exclusively depends on the parameters via the inner product $\mathbf{X}\boldsymbol{\theta}$. This will generally lead to $\mathbf{x}_\mathcal{A}^\top \boldsymbol{\theta}_\mathcal{A}^* \neq \mathbf{x}_\mathcal{B}^\top \boldsymbol{\theta}_\mathcal{B}^*$ for any two projections with the same kernel and different ranges.
2. **When not re-training the last layer:** applying the same parameters to projected embeddings that lie in two different subspaces will typically not lead to the same predictions. If we consider projections $\mathbf{P}_\mathcal{A}$ and $\mathbf{P}_\mathcal{B}$ with ranges \mathcal{A} and \mathcal{B} , then the predictions can only be the same if the parameters $\boldsymbol{\theta}^*$ lie in the orthogonal complement of both $\mathbf{P}_\mathcal{A}$ and $\mathbf{P}_\mathcal{B}$, i.e.,

$$\mathbf{x}^\top \mathbf{P}_\mathcal{A}^\top \boldsymbol{\theta}^* = \mathbf{x}^\top \mathbf{P}_\mathcal{B}^\top \boldsymbol{\theta}^* \Leftrightarrow \mathbf{x}^\top (\mathbf{P}_\mathcal{A} - \mathbf{P}_\mathcal{B})^\top \boldsymbol{\theta}^* = 0. \quad (6)$$

Since the projections considered in this paper are constructed without knowledge of the parameters, these will typically lie outside the orthogonal complements.

Note that this use case is relevant for language modeling, where re-training the parameters of the last layer is typically not feasible in terms of computational resources and/or data availability.

For these cases we expect SPLICE to outperform other methods that ensure linear guardedness, because it is explicitly designed to preserve task-relevant information. We empirically investigate this hypothesis in the next section.

4 Experiments

This section is structured as follows. We start by investigating classification tasks when the last layer of the model is re-fitted with regularization. Then, in Section 4.2, we investigate language modeling, when the last layer of the language model (LLM) is not re-trained post-projection. Finally, in order to qualitatively assess the effect of the different projections, we apply SPLICE to black and white image data in Section 4.3.

Across experiments, we compare SPLICE to two other projections: LEACE and SAL (see Section 2). We focus on these projections since, similar to SPLICE, they ensure linear guardedness with regards to a concept, and only differ in choice of range. Furthermore, LEACE and SAL have been shown to outperform other existing concept-removal methods such as INLP and RLACE.

4.1 Classification where the last layer is re-trained with regularization

We focus on two classification problems. First, we use the *Bias in Bios* dataset on professions and biographies from De-Arteaga et al. [2019]. We focus on the set of biographies which carry the ‘professor’ label, $y_{\text{prof}} \in \{0, 1\}$, and seek to remove the concept of whether the subject was male or not, $z_{\text{gender}} \in \{0, 1\}$. Second, inspired by Huang et al. [2024], we use the *Multilingual Text Detoxification* dataset from Dementieva et al. [2024]. We focus on three languages (English, German and French), making the concept-label $z_{\text{lang}} \in \{1, 2, 3\}$ non-binary. This dataset consists of texts from users that are classified as toxic or non-toxic, $y_{\text{tox}} \in \{0, 1\}$.

Set-up of the experiment: we seek to investigate the impact of each projection as the correlation between the task of interest ($y_{\text{prof}}, y_{\text{tox}}$) and the concept to remove ($z_{\text{gender}}, z_{\text{lang}}$) becomes stronger. We expect that as the relationship becomes stronger, the difference between SPLICE and other projections becomes greater. The reason is that stronger correlated labels have covariances with the embeddings that are typically more aligned. Removing the concept is then more likely to also remove information about the task of interest.

To alter the relationship between the task of interest and concept, we create smaller versions of the original datasets, where we vary the extent to which $y_{\text{prof}}, y_{\text{tox}}$ co-occur with respectively $z_{\text{gender}}, z_{\text{lang}}$. For the *Bias in Bios* dataset, we vary $p(y_{\text{prof}} = a \mid z_{\text{gender}} = a)$ with $a \in \{0, 1\}$, i.e., the conditional probability that the biography is of a professor and male or not a professor and female. For the *Multilingual Text Detoxification* dataset we vary $p(y_{\text{tox}} = 1 \mid z_{\text{lang}} = 1)$, e.g., the conditional probability that a toxic comment appears in the English language. We balance with respect to respectively $y_{\text{prof}}, y_{\text{tox}}$. In order to measure how much of the task-relevant information is retained after the projection, we create a test set where there is no correlation between $y_{\text{prof}}, y_{\text{tox}}$ and the respective concepts $z_{\text{gender}}, z_{\text{lang}}$. Additional details on the datasets are given in Appendix C.1.

Models and training procedure: for the *Bias in Bios* dataset, we finetune a BERT model [Devlin et al., 2019] to classify the profession. For the *Multilingual Text Detoxification* dataset we finetune multilingual E5 (ME5) embeddings Wang et al. [2024b] to classify the sentiment. For the BERT model, we add a linear layer on top of the embeddings of the [CLS] tokens for classification. For the ME5 embeddings, we add a linear layer on top of the average over all tokens. We apply projections to the last-layer embeddings - the [CLS] token for the BERT model, and the average over all tokens for the ME5 model. Afterwards we re-fit a logistic regression with l_2 regularization. We tune the strength of the l_2 regularization based on a validation set. This entire procedure (finetuning, projection, re-fitting, l_2 penalty selection) is repeated per seed. Additional details are given in Appendix C.2.

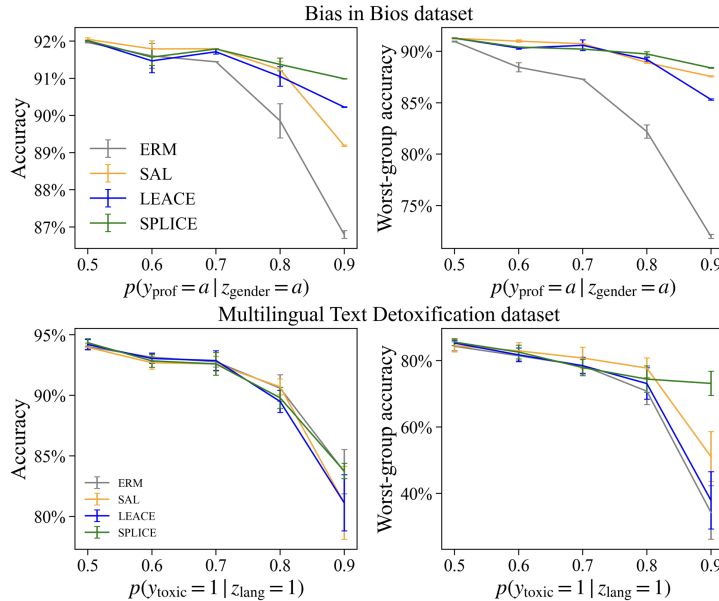


Figure 2: Performance of different projections on the *Bias in Bios* and *Multilingual Text Detoxification* dataset. We re-train the last-layer after applying each projection. Points are based on the average over 3 seeds, 5 seeds respectively for the two datasets. The error bars reflect the 95% confidence interval.

Results: the results of the experiments for both datasets are given in Figure 2. We focus on overall accuracy as well as worst-group accuracy. Worst-group accuracy is defined as the lowest accuracy for all combinations of the task and concept. A low worst-group accuracy reflects that a model relies on the correlation between the task and concept in the training data [Sagawa et al., 2020]. For both datasets, as the relationship between task and concept becomes stronger, SPLICE outperforms the other projections in both accuracy and worst-group accuracy. As the correlation between the task and concept becomes stronger, SAL and LEACE remove a significant part of $\Sigma_{x,y}$, contrary to SPLICE. This is illustrated for the *Bias in Bios* dataset in Figure 7 in Appendix B.2

4.2 Language modeling

We focus on two language modeling tasks. First, we use a dataset from Limisiewicz et al. [2024], which we refer to as the *profession dataset*. Inspired by Bolukbasi et al. [2016], this dataset contains prompt templates containing professions, which need to be finished by the LM (e.g., ‘the plumber wanted that’). Each profession has a *stereotype* score z_{stereo} . This indicates how strongly a profession is connected with the male gender through stereotypical cues (e.g., plumber has a high stereotype score, while nurse has a low one). Each profession also has a *factual* score y_{fact} , which indicates how strong a profession is connected to the male gender through factual information (e.g., waiter has a high factual score, but waitress has a low one).

Second, we use the *Winobias* dataset from Zhao et al. [2018]. Each prompt contains two professions and pronouns. Prompts are marked pro-stereotypical or anti-stereotypical, denoted $z_{\text{pro-stereo}} \in \{0, 1\}$. In pro-stereotypical prompts, the coreference links to a profession with the stereotypical gender matching the gender of the pronoun. An example is ‘The mechanic gave the clerk a present because he won the lottery. He refers to’. In anti-stereotypical cases, the profession’s stereotypically assumed gender is different from the gender of the pronouns. The task is to finish the prompt with one of the 40 professions, with the correct profession denoted $y_{\text{profession}} \in \{1, 2, \dots, 40\}$. For additional details on both datasets, see Appendix C.1.

Set-up of the experiments: for the *profession dataset*, our goal is to create an LM that does not rely on stereotypical cues, but on factual information. We estimate the extent to which the LM \mathcal{M} relies on stereotypical cues or factual information as follows. Let $t_{\text{he}}/t_{\text{she}}$ be the tokens for "he"/"she". Let t_i denote tokens for a prompt i , and $p_{\mathcal{M}}(t_{\text{he}}|t_i)$ the probability assigned by a model of the "he" token conditional on the prompt t_i . We measure the log-odds ratio between the probability of the next token being ‘he’ or ‘she’ as

$$\text{odds}_{\text{he/she},i} = \log \left(\frac{p_{\mathcal{M}}(t_{\text{he}}|t_i)}{p_{\mathcal{M}}(t_{\text{she}}|t_i)} \right), \quad (7)$$

and estimate the linear regression

$$\text{odds}_{\text{he/she},i} = z_{\text{stereo},i}\hat{\beta}_{\text{stereo}} + y_{\text{fact},i}\hat{\beta}_{\text{fact}} + \hat{\alpha}. \quad (8)$$

Intuitively, the coefficients indicate to what extent the difference in the probability of assigning "he" or "she" can be explained by stereotypical cues or factual information [Limisiewicz et al., 2024].

For the *Winobias dataset*, we seek to create an LM that is able to provide the correct profession, regardless of whether or not the coreference link is pro-stereotypical. We seek to remove $z_{\text{pro-stereo}}$ while preserving the covariance between the embeddings and $y_{\text{profession}}$.

Results: for the experiment on the *profession dataset*, the results are shown in Table 1. We report the exponent of the coefficients in Equation 7, as this tells us how more likely the ‘he’ token becomes relative to the ‘she’ token after a one-unit increase in either the stereotypical or factual score. After applying any of the three projections, the extent to which the model relies on stereotypical information is greatly reduced, per the reduction in $\exp(\hat{\beta}_{\text{stereo}})$. The extent to which the model relies on factual information after a projection is greatly reduced when applying SAL or LEACE, whereas it is increased or preserved after applying SPLICE.

Table 1: Results of applying different projections to the last layer of various Llama models for the *profession* dataset.

Model	Projection	$\exp(\hat{\beta}_{\text{stereo}})$	$\exp(\hat{\beta}_{\text{fact}})$
Llama 2 7B	Original	3,59	15,71
	+SAL	0,80	5,90
	+LEACE	0,85	12,14
	+SPLICE	0,79	24,27*
Llama 2 13B	Original	3,84	20,2
	+SAL	0,84	4,81
	+LEACE	0,88	16,32
	+SPLICE	0,81	33,24*
Llama 3 8B	Original	3,98	19,02
	+SAL	0,87	3,50
	+LEACE	0,88	7,68
	+SPLICE	0,82	13,43*

Note: the * indicates that difference between the factual coefficient of our projection and the factual coefficient of LEACE is statistically significant at the 1% level according to a one-tailed t -test. The exponent of the coefficients estimates how the odds ratio changes with a one-unit change in z_{stereo} and y_{fact} , respectively.

For the experiment on the *Winobias* dataset, the results are shown in Figure 3. For two out of three Llama models, SPLICE improves coreference accuracy more than the other projections. In particular, it strongly increases the accuracy for anti-stereotypical prompts.

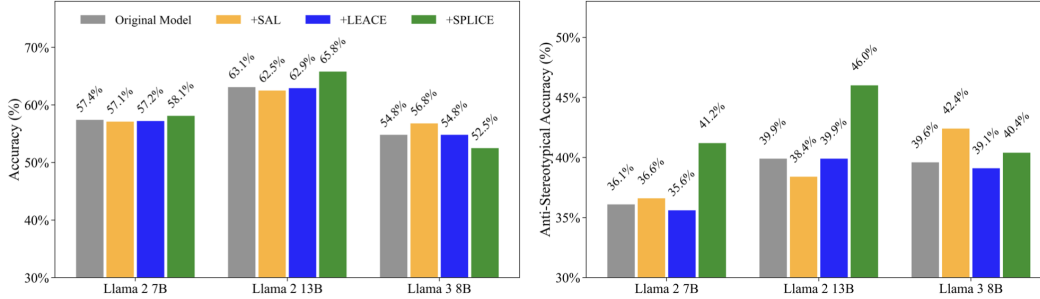


Figure 3: Results of applying different projections to the last layer of various Llama models for the *Winobias* dataset. The left plot shows the accuracy on a test set consisting of half pro-stereotypical and half anti-stereotypical prompts. The right plot shows the accuracy on the anti-stereotypical prompts in this test set.

4.3 Application to image data

We conduct an experiment for the *CelebA* dataset [Liu et al., 2015] that is similar to one from Ravfogel et al. [2022], Kleindessner et al. [2023], Holstege et al. [2024]. The goal of the experiment is to qualitatively show what features are removed by each projection. The concept to remove is whether or not someone is smiling, denoted $z_{\text{smiling}} \in \{0, 1\}$, and we seek to preserve whether or not someone wears glasses, $y_{\text{glasses}} \in \{0, 1\}$. We subsample 10,000 images from the original *CelebA* dataset such that $p(y_{\text{glasses}} = a \mid z_{\text{smiling}} = a) = 0.9$.

In Figure 4 we illustrate the effect of each projection on the raw pixels, for several images. SPLICE accentuates parts of the image that are useful for distinguishing images with and without glasses. For instance, it tends to make the areas around the eyes lighter when someone does not wear glasses, and darken when they do. This shows that SPLICE mitigates the damage to the “glasses” features exposed to a linear classifier, despite of the high correlation. We illustrate that this holds on average across the whole dataset in Appendix B.3.

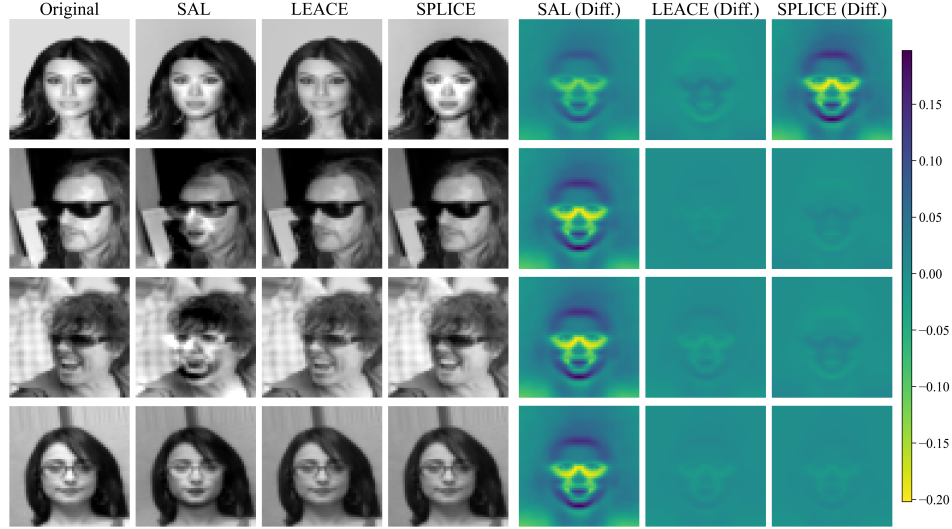


Figure 4: Application of different projections to raw pixel data of CelebA. The first columns shows the original image. The next four columns show the image, after the respective projection. The final three columns indicate the difference between the original image and the image after the projection.

5 Discussion and Limitations

Theoretically, we show that the range of the projection—particularly, whether or not it includes $\Sigma_{x,y}$ —can matter only if one does not re-fit the last linear layer, or refit it with a regularization term. However, we lack a theory that would explain under which conditions it *does* matter, and when it is expected to outperform LEACE. Future work should study whether preserving main-task covariance is optimal under some settings. In this paper, we focus on preserving that quantity as it is intuitively related to the desideratum of main-task performance; however, we note that the SPLICE objective can easily be modified to preserve *any* direction that is not identical to the covariance with the protected attribute.

In addition, a limitation of the SPLICE objective is that it prioritizes preserving $\Sigma_{x,y}$ over minimizing $\mathbb{E} [\|\mathbf{P}\mathbf{x} - \mathbf{x}\|_{\mathbf{M}}^2]$. This can potentially lead to distortive changes to the embeddings. We investigate this limitation in Appendix B.4. As the SPLICE objective sometimes fails when intervening in middle layers, we aim to study the adaption of the SPLICE objective for preserving the directions in the representation space that are being used by an LM in some middle layer.

6 Conclusion

We introduce SPLICE, a method that generalizes previous concept-erasure methods by provably removing the ability to linearly predict sensitive information, while maintaining the covariance between the representations and *another* main-task label. Our analysis pins the problem down to a pair of geometric constraints—placing $\text{colsp}(\Sigma_{x,z})$ in the kernel of the projection while forcing $\text{colsp}(\Sigma_{x,y})$ to lie in its range—and proves that the oblique projector of Theorem 1 is the unique minimum-distortion solution under these constraints. Experimentally, SPLICE tends to better preserve average and worst-group accuracy on the *Bias in Bios* and *Multilingual Text Detoxification* tasks when the task–concept correlation is high. In a language-modeling setting, we are able to influence stereotypical bias while preserving factual gender information; and in most models, it is better in preserving LM’s ability to perform co-reference after debiasing in the *Winobias* dataset. Future work should formalize whether maintaining the covariance with the main-task translates into main-task loss guarantees and develop variants over the SPLICE objective that impose weaker distortion when applied to earlier hidden layers.

References

- A. Albert and J. A. Anderson. On the Existence of Maximum Likelihood Estimates in Logistic Regression Models. *Biometrika*, 71(1):1–10, 1984. ISSN 0006-3444. doi: 10.2307/2336390.
- Andy Arditi, Oscar Obeso, Aaquib Syed, Daniel Paleka, Nina Panickssery, Wes Gurnee, and Neel Nanda. Refusal in language models is mediated by a single direction, 2024. URL <https://arxiv.org/abs/2406.11717>.
- Dilyara Bareeva, Maximilian Dreyer, Frederik Pahde, Wojciech Samek, and Sebastian Lapuschkin. Reactive model correction: Mitigating harm to task-relevant features via conditional bias suppression. *2024 IEEE/CVF Conference on Computer Vision and Pattern Recognition Workshops (CVPRW)*, pages 3532–3541, 2024. URL <https://api.semanticscholar.org/CorpusID:269148614>.
- Yonatan Belinkov. Probing classifiers: Promises, shortcomings, and advances. *Computational Linguistics*, 48(1):207–219, March 2022. doi: 10.1162/coli_a_00422. URL <https://aclanthology.org/2022.c1-1.7>.
- Nora Belrose, David Schneider-Joseph, Shauli Ravfogel, Ryan Cotterell, Edward Raff, and Stella Biderman. Leace: Perfect linear concept erasure in closed form. In A. Oh, T. Nauermann, A. Globerson, K. Saenko, M. Hardt, and S. Levine, editors, *Advances in Neural Information Processing Systems*, volume 36, pages 66044–66063. Curran Associates, Inc., 2023. URL https://proceedings.neurips.cc/paper_files/paper/2023/file/d066d21c619d0a78c5b557fa3291a8f4-Paper-Conference.pdf.
- Tolga Bolukbasi, Kai-Wei Chang, James Zou, Venkatesh Saligrama, and Adam Kalai. Man is to computer programmer as woman is to homemaker? debiasing word embeddings. In *Proceedings of the 30th International Conference on Neural Information Processing Systems, NIPS’16*, page 4356–4364, Red Hook, NY, USA, 2016. Curran Associates Inc. ISBN 9781510838819.
- Hongliu Cao. Recent advances in text embedding: A comprehensive review of top-performing methods on the mteb benchmark, 2024. URL <https://arxiv.org/abs/2406.01607>.
- Maria De-Arteaga, Alexey Romanov, Hanna Wallach, Jennifer Chayes, Christian Borgs, Alexandra Chouldechova, Sahin Geyik, Krishnaram Kenthapadi, and Adam Tauman Kalai. Bias in bios: A case study of semantic representation bias in a high-stakes setting. In *Proceedings of the Conference on Fairness, Accountability, and Transparency, FAT* ’19*, page 120–128, New York, NY, USA, 2019. Association for Computing Machinery. ISBN 9781450361255. doi: 10.1145/3287560.3287572. URL <https://doi.org/10.1145/3287560.3287572>.
- Daryna Dementieva, Daniil Moskovskiy, Nikolay Babakov, Abinew Ali Ayele, Naqee Rizwan, Froilan Schneider, Xintong Wang, Seid Muhie Yimam, Dmitry Ustalov, Elisei Stakovskii, Alisa Smirnova, Ashraf Elnagar, Animesh Mukherjee, and Alexander Panchenko. Overview of the multilingual text detoxification task at pan 2024. In Guglielmo Faggioli, Nicola Ferro, Petra Galuščáková, and Alba García Seco de Herrera, editors, *Working Notes of CLEF 2024 - Conference and Labs of the Evaluation Forum*. CEUR-WS.org, 2024.
- Sunipa Dev, Tao Li, Jeff M Phillips, and Vivek Srikumar. OSCaR: Orthogonal subspace correction and rectification of biases in word embeddings. In Marie-Francine Moens, Xuanjing Huang, Lucia Specia, and Scott Wen-tau Yih, editors, *Proceedings of the 2021 Conference on Empirical Methods in Natural Language Processing*, pages 5034–5050, Online and Punta Cana, Dominican Republic, November 2021. Association for Computational Linguistics. doi: 10.18653/v1/2021.emnlp-main.411. URL <https://aclanthology.org/2021.emnlp-main.411/>.
- Jacob Devlin, Ming-Wei Chang, Kenton Lee, and Kristina Toutanova. BERT: Pre-training of deep bidirectional transformers for language understanding. In Jill Burstein, Christy Doran, and Tamar Solorio, editors, *Proceedings of the 2019 Conference of the North American Chapter of the Association for Computational Linguistics: Human Language Technologies, Volume 1 (Long and Short Papers)*, pages 4171–4186, Minneapolis, Minnesota, June 2019. Association for Computational Linguistics. doi: 10.18653/v1/N19-1423. URL <https://aclanthology.org/N19-1423/>.

- Yanai Elazar and Yoav Goldberg. Adversarial removal of demographic attributes from text data. In Ellen Riloff, David Chiang, Julia Hockenmaier, and Jun’ichi Tsujii, editors, *Proceedings of the 2018 Conference on Empirical Methods in Natural Language Processing*, pages 11–21, Brussels, Belgium, October–November 2018. Association for Computational Linguistics. doi: 10.18653/v1/D18-1002. URL <https://aclanthology.org/D18-1002/>.
- Amir Feder, Nadav Oved, Uri Shalit, and Roi Reichart. Causalm: Causal model explanation through counterfactual language models. *Computational Linguistics*, 47(2):333–386, 2021.
- Clément Guerner, Tianyu Liu, Anej Svete, Alexander Warstadt, and Ryan Cotterell. A geometric notion of causal probing, 2025. URL <https://arxiv.org/abs/2307.15054>.
- Pantea Haghighathkhan, Antske Fokkens, Pia Sommerauer, Bettina Speckmann, and Kevin Verbeek. Better hit the nail on the head than beat around the bush: Removing protected attributes with a single projection. In Yoav Goldberg, Zornitsa Kozareva, and Yue Zhang, editors, *Proceedings of the 2022 Conference on Empirical Methods in Natural Language Processing*, pages 8395–8416, Abu Dhabi, United Arab Emirates, December 2022. Association for Computational Linguistics. doi: 10.18653/v1/2022.emnlp-main.575. URL <https://aclanthology.org/2022.emnlp-main.575/>.
- Floris Holstege, Bram Wouters, Noud Van Giersbergen, and Cees Diks. Removing spurious concepts from neural network representations via joint subspace estimation. In Ruslan Salakhutdinov, Zico Kolter, Katherine Heller, Adrian Weller, Nuria Oliver, Jonathan Scarlett, and Felix Berkenkamp, editors, *Proceedings of the 41st International Conference on Machine Learning*, volume 235 of *Proceedings of Machine Learning Research*, pages 18568–18610. PMLR, 21–27 Jul 2024. URL <https://proceedings.mlr.press/v235/holstege24a.html>.
- Zhiqi Huang, Puxuan Yu, Shauli Ravfogel, and James Allan. Language concept erasure for language-invariant dense retrieval. In Yaser Al-Onaizan, Mohit Bansal, and Yun-Nung Chen, editors, *Proceedings of the 2024 Conference on Empirical Methods in Natural Language Processing*, pages 13261–13273, Miami, Florida, USA, November 2024. Association for Computational Linguistics. doi: 10.18653/v1/2024.emnlp-main.736. URL <https://aclanthology.org/2024.emnlp-main.736/>.
- Matthäus Kleindessner, Michele Donini, Chris Russell, and Muhammad Bilal Zafar. Efficient fair pca for fair representation learning. In Francisco Ruiz, Jennifer Dy, and Jan-Willem van de Meent, editors, *Proceedings of The 26th International Conference on Artificial Intelligence and Statistics*, volume 206 of *Proceedings of Machine Learning Research*, pages 5250–5270. PMLR, 25–27 Apr 2023. URL <https://proceedings.mlr.press/v206/kleindessner23a.html>.
- Abhinav Kumar, Chenhao Tan, and Amit Sharma. Probing classifiers are unreliable for concept removal and detection. In S. Koyejo, S. Mohamed, A. Agarwal, D. Belgrave, K. Cho, and A. Oh, editors, *Advances in Neural Information Processing Systems*, volume 35, pages 17994–18008. Curran Associates, Inc., 2022. URL https://proceedings.neurips.cc/paper_files/paper/2022/file/725f5e8036cc08adeba4a7c3bcbcf2c-Paper-Conference.pdf.
- Tomasz Limisiewicz, David Mareček, and Tomáš Musil. Debiasing algorithm through model adaptation, 2024. URL <https://arxiv.org/abs/2310.18913>.
- Tomasz Limisiewicz, David Mareček, and Tomáš Musil. Dual debiasing: Remove stereotypes and keep factual gender for fair language modeling and translation, 2025. URL <https://arxiv.org/abs/2501.10150>.
- Ziwei Liu, Ping Luo, Xiaogang Wang, and Xiaoou Tang. Deep learning face attributes in the wild. In *Proceedings of International Conference on Computer Vision (ICCV)*, December 2015.
- Ilya Loshchilov and Frank Hutter. Decoupled weight decay regularization, 2019. URL <https://arxiv.org/abs/1711.05101>.
- Kiho Park, Yo Joong Choe, and Victor Veitch. The linear representation hypothesis and the geometry of large language models. In Ruslan Salakhutdinov, Zico Kolter, Katherine Heller, Adrian Weller, Nuria Oliver, Jonathan Scarlett, and Felix Berkenkamp, editors, *Proceedings of the 41st International Conference on Machine Learning*, volume 235 of *Proceedings of*

- Machine Learning Research*, pages 39643–39666. PMLR, 21–27 Jul 2024. URL <https://proceedings.mlr.press/v235/park24c.html>.
- Shauli Ravfogel, Yanai Elazar, Hila Gonen, Michael Twiton, and Yoav Goldberg. Null it out: Guarding protected attributes by iterative nullspace projection. In *Proceedings of the 58th Annual Meeting of the Association for Computational Linguistics*, pages 7237–7256, Online, July 2020. Association for Computational Linguistics. doi: 10.18653/v1/2020.acl-main.647. URL <https://aclanthology.org/2020.acl-main.647>.
- Shauli Ravfogel, Michael Twiton, Yoav Goldberg, and Ryan D Cotterell. Linear adversarial concept erasure. In Kamalika Chaudhuri, Stefanie Jegelka, Le Song, Csaba Szepesvari, Gang Niu, and Sivan Sabato, editors, *Proceedings of the 39th International Conference on Machine Learning*, volume 162 of *Proceedings of Machine Learning Research*, pages 18400–18421. PMLR, 17–23 Jul 2022. URL <https://proceedings.mlr.press/v162/ravfogel22a.html>.
- Shauli Ravfogel, Yoav Goldberg, and Ryan Cotterell. Log-linear Guardedness and its Implications. In Anna Rogers, Jordan Boyd-Graber, and Naoaki Okazaki, editors, *Proceedings of the 61st Annual Meeting of the Association for Computational Linguistics (Volume 1: Long Papers)*, pages 9413–9431, Toronto, Canada, 2023. Association for Computational Linguistics. doi: 10.18653/v1/2023.acl-long.523.
- Shauli Ravfogel, Anej Svete, Vésteinn Snæbjarnarson, and Ryan Cotterell. Gumbel counterfactual generation from language models, 2025. URL <https://arxiv.org/abs/2411.07180>.
- Shiori Sagawa, Pang Wei Koh, Tatsunori B Hashimoto, and Percy Liang. Distributionally robust neural networks for group shifts: On the importance of regularization for worst-case generalization. In *International Conference on Learning Representations (ICLR)*, 2020.
- Shun Shao, Yftah Ziser, and Shay B. Cohen. Gold doesn’t always glitter: Spectral removal of linear and nonlinear guarded attribute information. In Andreas Vlachos and Isabelle Augenstein, editors, *Proceedings of the 17th Conference of the European Chapter of the Association for Computational Linguistics*, pages 1611–1622, Dubrovnik, Croatia, May 2023. Association for Computational Linguistics. doi: 10.18653/v1/2023.eacl-main.118. URL <https://aclanthology.org/2023.eacl-main.118>.
- Aili Shen, Xudong Han, Trevor Cohn, Timothy Baldwin, and Lea Frermann. Contrastive learning for fair representations. *arXiv preprint arXiv:2109.10645*, 2021.
- Enze Shi, Lei Ding, Linglong Kong, and Bei Jiang. Debiasing with sufficient projection: A general theoretical framework for vector representations. In Kevin Duh, Helena Gomez, and Steven Bethard, editors, *Proceedings of the 2024 Conference of the North American Chapter of the Association for Computational Linguistics: Human Language Technologies (Volume 1: Long Papers)*, pages 5960–5975, Mexico City, Mexico, June 2024. Association for Computational Linguistics. doi: 10.18653/v1/2024.naacl-long.332. URL <https://aclanthology.org/2024.naacl-long.332/>.
- Liang Wang, Nan Yang, Xiaolong Huang, Linjun Yang, Rangan Majumder, and Furu Wei. Improving text embeddings with large language models, 2024a. URL <https://arxiv.org/abs/2401.00368>.
- Liang Wang, Nan Yang, Xiaolong Huang, Linjun Yang, Rangan Majumder, and Furu Wei. Multilingual e5 text embeddings: A technical report, 2024b. URL <https://arxiv.org/abs/2402.05672>.
- Thomas Wolf, Lysandre Debut, Victor Sanh, Julien Chaumond, Clement Delangue, Anthony Moi, Pierric Cistac, Tim Rault, Rémi Louf, Morgan Funtowicz, and Jamie Brew. Huggingface’s transformers: State-of-the-art natural language processing. *CoRR*, abs/1910.03771, 2019. URL <http://arxiv.org/abs/1910.03771>.
- Qizhe Xie, Zihang Dai, Yulun Du, Eduard Hovy, and Graham Neubig. Controllable invariance through adversarial feature learning. In *Proceedings of the 31st International Conference on Neural Information Processing Systems*, NIPS’17, page 585–596, Red Hook, NY, USA, 2017. Curran Associates Inc. ISBN 9781510860964.

Brian Hu Zhang, Blake Lemoine, and Margaret Mitchell. Mitigating unwanted biases with adversarial learning. In *Proceedings of the 2018 AAAI/ACM Conference on AI, Ethics, and Society*, AIES '18, page 335–340, New York, NY, USA, 2018. Association for Computing Machinery. ISBN 9781450360128. doi: 10.1145/3278721.3278779. URL <https://doi.org/10.1145/3278721.3278779>.

Jieyu Zhao, Tianlu Wang, Mark Yatskar, Vicente Ordonez, and Kai-Wei Chang. Gender bias in coreference resolution: Evaluation and debiasing methods. In Marilyn Walker, Heng Ji, and Amanda Stent, editors, *Proceedings of the 2018 Conference of the North American Chapter of the Association for Computational Linguistics: Human Language Technologies, Volume 2 (Short Papers)*, pages 15–20, New Orleans, Louisiana, June 2018. Association for Computational Linguistics. doi: 10.18653/v1/N18-2003. URL <https://aclanthology.org/N18-2003/>.

A Proofs of theorems

A.1 Proof of theorem 1

We will prove Theorem 1 by making use of a basis tailored to the problem. In the end we will transform the resulting formula back to the basis-independent formulation of equation 4.

Let $m = \text{rank}(\Sigma_{\mathbf{x}, \mathbf{x}})$, with $1 \leq m \leq d$. Let $\mathcal{W} = \text{colsp}(\mathbf{W})$ be the subspace in \mathbb{R}^d in which \mathbf{x} has non-zero variance. Without loss of generality, we will define a basis for \mathbf{x} where the first m coordinates of \mathbf{x} lie in \mathcal{W} . The last $l = d - m$ coordinates lie in its orthogonal complement \mathcal{W}^\perp . Our \mathbf{x} can now be written as

$$\mathbf{x} = \begin{pmatrix} \tilde{\mathbf{x}} \\ \check{\mathbf{x}} \end{pmatrix}, \quad \tilde{\mathbf{x}} \in \mathbb{R}^m, \check{\mathbf{x}} \in \mathbb{R}^l. \quad (9)$$

We will use $\tilde{x}_i \in \mathbb{R}$ to denote elements from the first m coordinates, and $\check{x}_i \in \mathbb{R}$ to denote elements from the final l coordinates.

We also assume that this basis is orthonormal with respect to the inner product \mathbf{M} , such that: $\mathbf{x}^\top \mathbf{M} \mathbf{x} = \sum_{i=1}^d \alpha_i x_i^2$ for fixed $\alpha_1, \dots, \alpha_d > 0$. Creating such a basis is always possible by standard orthogonalization procedures, now restricted to the coordinates of the respective subspaces \mathcal{W} and \mathcal{W}^\perp . As a consequence of this, the optimization problem defined in Theorem 1 can be decomposed in d independent optimization problems, one for each term in the sum that corresponds to the norm (squared), i.e., one for each coordinate of \mathbf{x} . To be more concrete, the optimization problem becomes for $i \in \{1, \dots, d\}$

$$\begin{aligned} \arg \min_{\mathbf{P} \in \mathbb{R}^{d \times d}} \mathbb{E} [((\mathbf{P}\mathbf{x})_i - x_i)^2] \quad \text{subject to } \text{Cov}((\mathbf{P}\mathbf{x})_i, \mathbf{z}) = \mathbf{0}, \\ \text{subject to } \text{Cov}((\mathbf{P}\mathbf{x})_i, \mathbf{y}) = \text{Cov}(x_i, \mathbf{y}), \end{aligned} \quad (10)$$

where $x_i \in \mathbb{R}$ denotes the i^{th} component of \mathbf{x} and $(\mathbf{P}\mathbf{x})_i \in \mathbb{R}$ the i^{th} component of $\mathbf{P}\mathbf{x}$. The weights $\alpha_1, \dots, \alpha_d$ are left out, as they become irrelevant if we manage to find the minimum for each x_i .

Lemma 1. *Let*

$$\mathbf{P} = \begin{pmatrix} \tilde{\mathbf{P}} & \mathbf{0}_{m,l} \\ \mathbf{0}_{l,m} & \mathbf{0}_{l,l} \end{pmatrix}, \quad (11)$$

where $\tilde{\mathbf{P}} \in \mathbb{R}^{m \times m}$ and where $\mathbf{0}_{m,l}$ is an $(m \times l)$ -matrix of zeros and the other zero-matrices are defined similarly. A solution to the optimization problem, for $i \in \{1, \dots, m\}$,

$$\begin{aligned} \arg \min_{\tilde{\mathbf{P}} \in \mathbb{R}^{d \times d}} \mathbb{E} [((\tilde{\mathbf{P}}\tilde{\mathbf{x}})_i - \tilde{x}_i)^2] \quad \text{subject to } \text{Cov}((\tilde{\mathbf{P}}\tilde{\mathbf{x}})_i, \mathbf{z}) = \mathbf{0}, \\ \text{subject to } \text{Cov}((\tilde{\mathbf{P}}\tilde{\mathbf{x}})_i, \mathbf{y}) = \text{Cov}(\tilde{x}_i, \mathbf{y}), \end{aligned} \quad (12)$$

corresponds then via equation 11 to a solution of the original optimization problem of Theorem 1.

Proof. We start by dividing \mathbf{P} in four block matrices,

$$\mathbf{P} = \begin{pmatrix} \tilde{\mathbf{P}} & \mathbf{B} \\ \mathbf{C} & \mathbf{D} \end{pmatrix}, \quad (13)$$

where $\tilde{\mathbf{P}} \in \mathbb{R}^{m \times m}$, $\mathbf{B} \in \mathbb{R}^{m \times l}$, $\mathbf{C} \in \mathbb{R}^{l \times m}$, $\mathbf{D} \in \mathbb{R}^{l \times l}$. We now proceed to determine these matrices, starting with a solution for \mathbf{C} and \mathbf{D} . We do this by solving the optimization problem defined in equation 10 for the final l rows. For $i \in \{l, \dots, d\}$, we can write

$$(\mathbf{P}\mathbf{x})_i = \sum_{j=1}^m C_{p,j} \tilde{x}_j + \sum_{j=m+1}^d D_{p,j} \check{x}_j, \quad (14)$$

where $p = i - l + 1$. We use the indexation via p because we use the rows $p \in \{1, \dots, l\}$ of the matrices \mathbf{C} and \mathbf{D} respectively to represent $(\mathbf{P}\mathbf{x})_i$. The objective in equation 10 for $i \in \{l, \dots, d\}$

and corresponding p can be written as

$$\mathbb{E} [((\mathbf{P}\mathbf{x})_i - \tilde{x}_i)^2] = \mathbb{E} \left[\left(\sum_{j=1}^m C_{p,j} \tilde{x}_j + \sum_{j=m+1}^d D_{p,j} \tilde{x}_j - \tilde{x}_i \right)^2 \right] \quad (15)$$

$$= \mathbb{E} \left[\sum_{j=1}^m C_{p,j} \tilde{x}_j \right]^2 \quad (16)$$

$$= \left(\mathbf{C} \text{Cov}(\tilde{\mathbf{x}}, \tilde{\mathbf{x}}) \mathbf{C}^T \right)_{pp}, \quad (17)$$

where in the second equality we used that $\tilde{x}_i = 0$ almost surely and in the final equality we used that $\mathbb{E}[\tilde{x}_i] = 0$. We note that the values for $D_{p,j}$ do not matter for the objective. Further, because $\text{Cov}(\tilde{\mathbf{x}}, \tilde{\mathbf{x}})$ is p.s.d., we can achieve the minimum of equation 17 by setting $\mathbf{C} = \mathbf{0}$. For simplicity, we also set $\mathbf{D} = \mathbf{0}$. This then also trivially satisfies the kernel and range constraints for the components $i \in \{l, \dots, d\}$.

For $i \in \{1, \dots, m\}$, we can write

$$(\mathbf{P}\mathbf{x})_i = \sum_{j=1}^m A_{i,j} \tilde{x}_j + \sum_{j=m+1}^d B_{i,j} \tilde{x}_j. \quad (18)$$

We can set $\mathbf{B} = \mathbf{0}$ for the same reason as we chose $\mathbf{D} = \mathbf{0}$. The objective and constraints for $\tilde{\mathbf{P}}$ are then as in equation 12. This concludes the proof of Lemma 1. \square

In order to simplify the remaining objective for $\tilde{\mathbf{P}}$ in Lemma 1, we write $\tilde{\mathbf{P}} = \tilde{\mathbf{A}}\tilde{\mathbf{W}}$, where $\tilde{\mathbf{W}} = \Sigma_{\tilde{\mathbf{x}}, \tilde{\mathbf{x}}} \in \mathbb{R}^{m \times m}$ is full-rank, symmetric and p.s.d., and thus invertible. Because of this, optimizing for $\tilde{\mathbf{P}}$ is equivalent to optimizing for $\tilde{\mathbf{A}}$. Note that in this notation,

$$\Sigma_{\mathbf{x}, \mathbf{x}} = \begin{pmatrix} \Sigma_{\tilde{\mathbf{x}}, \tilde{\mathbf{x}}} & \mathbf{0}_{m,l} \\ \mathbf{0}_{l,m} & \mathbf{0}_{l,l} \end{pmatrix}, \quad (19)$$

an we can write the whitening matrix \mathbf{W} , and its Moore-Penrose inverse as

$$\mathbf{W} = \begin{pmatrix} \tilde{\mathbf{W}} & \mathbf{0}_{m,l} \\ \mathbf{0}_{l,m} & \mathbf{0}_{l,l} \end{pmatrix}, \quad \mathbf{W}^+ = \begin{pmatrix} \tilde{\mathbf{W}}^{-1} & \mathbf{0}_{m,l} \\ \mathbf{0}_{l,m} & \mathbf{0}_{l,l} \end{pmatrix}. \quad (20)$$

Using that we can write \tilde{x}_i as

$$\tilde{x}_i = (\tilde{\mathbf{W}}^{-1} \tilde{\mathbf{W}} \tilde{\mathbf{x}})_i = \sum_{j=1}^m \tilde{W}_{i,j}^{-1} (\tilde{\mathbf{W}} \tilde{\mathbf{x}})_j, \quad (21)$$

the remaining objective becomes, for $i \in \{1, \dots, m\}$,

$$\begin{aligned}
\mathbb{E} [((\mathbf{P}\mathbf{x})_i - \tilde{x}_i)^2] &= \mathbb{E} [((\tilde{\mathbf{P}}\tilde{\mathbf{x}})_i - \tilde{x}_i)^2] \\
&= \mathbb{E} \left[\left(\sum_{j=1}^m (\tilde{\mathbf{A}}_{i,j} - \tilde{\mathbf{W}}_{i,j}^{-1})(\tilde{\mathbf{W}}\tilde{\mathbf{x}})_j \right)^2 \right] \\
&= \text{Var} \left(\sum_{j=1}^m (\tilde{\mathbf{A}}_{i,j} - \tilde{\mathbf{W}}_{i,j}^{-1})(\tilde{\mathbf{W}}\tilde{\mathbf{x}})_j \right) + \mathbb{E} \left[\sum_{j=1}^m (\tilde{\mathbf{A}}_{i,j} - \tilde{\mathbf{W}}_{i,j}^{-1})(\tilde{\mathbf{W}}\tilde{\mathbf{x}})_j \right]^2 \\
&= \text{Var} \left(\sum_{j=1}^m (\tilde{\mathbf{A}}_{i,j} - \tilde{\mathbf{W}}_{i,j}^{-1})(\tilde{\mathbf{W}}\tilde{\mathbf{x}})_j \right) \\
&= \sum_{h=1}^m \sum_{k=1}^m (\tilde{\mathbf{A}}_{i,h} - \tilde{\mathbf{W}}_{i,h}^{-1})(\tilde{\mathbf{A}}_{i,k} - \tilde{\mathbf{W}}_{i,k}^{-1}) \text{Cov}((\tilde{\mathbf{W}}\tilde{\mathbf{x}})_h, (\tilde{\mathbf{W}}\tilde{\mathbf{x}})_k) \\
&= \left[(\tilde{\mathbf{A}} - \tilde{\mathbf{W}}^{-1}) (\tilde{\mathbf{A}} - \tilde{\mathbf{W}}^{-1})^T \right]_{i,i}, \tag{22}
\end{aligned}$$

where we used that $\mathbb{E}[(\tilde{\mathbf{W}}\tilde{\mathbf{x}})_j] = 0$ and $\text{Cov}(\tilde{\mathbf{W}}\tilde{\mathbf{x}}, \tilde{\mathbf{W}}\tilde{\mathbf{x}}) = \mathbf{I}_m$ by definition of the whitening matrix.

The constraints on $\tilde{\mathbf{P}}$ in the optimization problem in equation 12 translate into constraints on $\tilde{\mathbf{A}}$ and the optimization problem can be recast as

$$\tilde{\mathbf{A}}^* = \arg \min_{\tilde{\mathbf{A}} \in \mathcal{C}_1 \cap \mathcal{C}_2} \left\{ \sum_{j=1}^m \left(\tilde{\mathbf{A}} - \tilde{\mathbf{W}}^{-1} \right)_{i,j}^2 \right\}_{i=1}^m, \tag{23a}$$

where

$$\mathcal{C}_1 = \left\{ M \in \mathbb{R}^{m \times m} \mid \tilde{\mathbf{W}} M \tilde{\mathbf{W}} \Sigma_{\tilde{\mathbf{x}}, \mathbf{z}} = \mathbf{0}_m \right\}, \tag{23b}$$

$$\mathcal{C}_2 = \left\{ M \in \mathbb{R}^{m \times m} \mid \tilde{\mathbf{W}} M \tilde{\mathbf{W}} \Sigma_{\tilde{\mathbf{x}}, \mathbf{y}} = \tilde{\mathbf{W}} \Sigma_{\tilde{\mathbf{x}}, \mathbf{y}} \right\}. \tag{23c}$$

With more than one objective and two constraints, this is a constrained multiple optimization problem. We have seen before that it can be decomposed in m separate constrained optimization problems. Each of these problems has a convex objective function and linear constraints, making the optimum $\tilde{\mathbf{A}}^*$ uniquely defined.

The constraints \mathcal{C}_1 and \mathcal{C}_2 can be interpreted as follows: $\tilde{\mathbf{A}}$ must be such that the columns of $\tilde{\mathbf{W}} \Sigma_{\tilde{\mathbf{x}}, \mathbf{z}}$ are in the kernel of $\tilde{\mathbf{W}} \tilde{\mathbf{A}}$ and that the columns of $\tilde{\mathbf{W}} \Sigma_{\tilde{\mathbf{x}}, \mathbf{y}}$ are eigenvectors of $\tilde{\mathbf{W}} \tilde{\mathbf{A}}$. This can be achieved by means of an oblique projection. If we define the following linear subspaces,

$$\tilde{\mathcal{U}}^\perp = \text{colsp}(\tilde{\mathbf{W}} \Sigma_{\tilde{\mathbf{x}}, \mathbf{z}}), \tag{24}$$

$$\tilde{\mathcal{U}}^- = \tilde{\mathcal{U}} \cap \left(\text{colsp}(\tilde{\mathbf{W}} \Sigma_{\tilde{\mathbf{x}}, \mathbf{z}}) + \text{colsp}(\tilde{\mathbf{W}} \Sigma_{\tilde{\mathbf{x}}, \mathbf{y}}) \right)^\perp, \tag{25}$$

$$\tilde{\mathcal{V}} = \text{colsp}(\tilde{\mathbf{W}} \Sigma_{\tilde{\mathbf{x}}, \mathbf{y}}) + \tilde{\mathcal{U}}^-, \tag{26}$$

and we define $\tilde{\mathbf{U}}$ and $\tilde{\mathbf{V}}$ as the matrices whose columns are an orthonormal basis of $\tilde{\mathcal{U}}$ and $\tilde{\mathcal{V}}$, respectively, then

$$\tilde{\mathbf{P}}_{\text{obl}} = \tilde{\mathbf{V}} \left(\tilde{\mathbf{U}}^T \tilde{\mathbf{V}} \right)^{-1} \tilde{\mathbf{U}}^T \tag{27}$$

is the transformation matrix of an oblique projection whose kernel is formed by the columns of $\tilde{\mathbf{W}} \Sigma_{\tilde{\mathbf{x}}, \mathbf{z}}$ and whose range include the columns of $\tilde{\mathbf{W}} \Sigma_{\tilde{\mathbf{x}}, \mathbf{y}}$. The latter means that the columns of $\tilde{\mathbf{W}} \Sigma_{\tilde{\mathbf{x}}, \mathbf{y}}$ are eigenvectors of $\tilde{\mathbf{P}}_{\text{obl}}$.

We claim that any $\tilde{\mathbf{A}} \in \mathcal{C}_1 \cap \mathcal{C}_2$ can be written as $\tilde{\mathbf{B}} \tilde{\mathbf{P}}_{\text{obl}}$, where $\tilde{\mathbf{B}}$ obeys the second constraint, i.e., $\tilde{\mathbf{B}} \in \mathcal{C}_2$. This identification is not unique, as multiple $\tilde{\mathbf{B}}$ lead to the same $\tilde{\mathbf{A}}$. We formalize this claim in the following lemma.

Lemma 2. *Let us define*

$$\mathcal{B}_{\tilde{\mathbf{P}}_{\text{obl}}} := \left\{ \tilde{\mathbf{B}}\tilde{\mathbf{P}}_{\text{obl}} \mid \tilde{\mathbf{B}} \in \mathcal{C}_2 \right\}. \quad (28)$$

Then $\mathcal{B}_{\tilde{\mathbf{P}}_{\text{obl}}} = \mathcal{C}_1 \cap \mathcal{C}_2$.

Proof. It is obvious that $\mathcal{B}_{\tilde{\mathbf{P}}_{\text{obl}}} \subseteq \mathcal{C}_1 \cap \mathcal{C}_2$, so we focus on proving that $\mathcal{C}_1 \cap \mathcal{C}_2 \subseteq \mathcal{B}_{\tilde{\mathbf{P}}_{\text{obl}}}$. For this, take an arbitrary $\mathbf{M} \in \mathcal{C}_1 \cap \mathcal{C}_2$. Let

$$\left\{ \text{colsp}(\tilde{\mathbf{W}}\Sigma_{\tilde{\mathbf{x}},\mathbf{z}}), \text{colsp}(\tilde{\mathbf{W}}\Sigma_{\tilde{\mathbf{x}},\mathbf{y}}), w_1, w_2, \dots, w_k \right\}$$

be a basis of \mathbb{R}^m , where the $w_j \in \mathbb{R}^m$ are mutually orthonormal and orthogonal to $\tilde{\mathbf{W}}\Sigma_{\tilde{\mathbf{x}},\mathbf{z}}$ and $\tilde{\mathbf{W}}\Sigma_{\tilde{\mathbf{x}},\mathbf{y}}$. We then define a matrix $\tilde{\mathbf{B}} \in \mathbb{R}^{m \times m}$ in terms of its action on this basis, i.e.,

$$\begin{cases} \tilde{\mathbf{B}}\tilde{\mathbf{W}}\Sigma_{\tilde{\mathbf{x}},\mathbf{z}} = \mathbf{0}, \\ \tilde{\mathbf{B}}\tilde{\mathbf{W}}\Sigma_{\tilde{\mathbf{x}},\mathbf{y}} = \tilde{\mathbf{W}}^{-1}\tilde{\mathbf{W}}\Sigma_{\tilde{\mathbf{x}},\mathbf{y}}, \\ \tilde{\mathbf{B}}w_j = \mathbf{M}w_j, \quad j = 1, 2, \dots, k. \end{cases}$$

This implies that $\mathbf{M} = \tilde{\mathbf{B}}\tilde{\mathbf{P}}_{\text{obl}}$ and that $\tilde{\mathbf{B}} \in \mathcal{C}_2$. This concludes the proof of the lemma. \square

Lemma 2 enables us to reformulate the optimization problem of equation 23 as follows. Define the set

$$\mathcal{B}^* = \arg \min_{\tilde{\mathbf{B}} \in \mathcal{C}_2} \left\{ \left[\left(\tilde{\mathbf{B}}\tilde{\mathbf{P}}_{\text{obl}} - \tilde{\mathbf{W}}^{-1} \right) \left(\tilde{\mathbf{B}}\tilde{\mathbf{P}}_{\text{obl}} - \tilde{\mathbf{W}}^{-1} \right)^T \right]_{i,i} \right\}_{i=1}^m. \quad (29)$$

This is a set of solutions to a different constrained optimization problem than equation 23. All solutions are equivalent in the sense that for any $\tilde{\mathbf{B}}_1^*, \tilde{\mathbf{B}}_2^* \in \mathcal{B}^*$ we have that $\tilde{\mathbf{B}}_1^*\tilde{\mathbf{P}}_{\text{obl}} = \tilde{\mathbf{B}}_2^*\tilde{\mathbf{P}}_{\text{obl}}$. Seen as an optimization for $\tilde{\mathbf{B}}\tilde{\mathbf{P}}_{\text{obl}}$, the objective is convex and the constraints are linear, making the optimum unique. Hence, $\tilde{\mathbf{A}}^* = \tilde{\mathbf{B}}^*\tilde{\mathbf{P}}_{\text{obl}}$ for any $\tilde{\mathbf{B}}^* \in \mathcal{B}^*$.

Now, we claim that $\tilde{\mathbf{W}}^{-1} \in \mathcal{B}^*$. The argument is that $\tilde{\mathbf{W}}^{-1}$ is a solution to the unconstrained equivalent of the optimization problem of equation 29 and, conveniently, also obeys the constraint \mathcal{C}_2 . To see this, define

$$\mathcal{L}_i = \left[\left(\tilde{\mathbf{B}}\tilde{\mathbf{P}}_{\text{obl}} - \tilde{\mathbf{W}}^{-1} \right) \left(\tilde{\mathbf{B}}\tilde{\mathbf{P}}_{\text{obl}} - \tilde{\mathbf{W}}^{-1} \right)^T \right]_{i,i}, \quad (30)$$

for $i \in \{1, \dots, m\}$, and take the derivative of the loss function with respect to elements of $\tilde{\mathbf{B}}$,

$$\frac{\partial \mathcal{L}_i}{\partial \tilde{\mathbf{B}}_{i,k}} = 2 \left(\left(\tilde{\mathbf{B}} - \tilde{\mathbf{W}}^{-1} \right) \tilde{\mathbf{P}}_{\text{obl}} \right)_{i,k}, \quad (31)$$

where we used that $\tilde{\mathbf{P}}_{\text{obl}}$ is idempotent. One solution to these first order conditions is $\tilde{\mathbf{B}} = \tilde{\mathbf{W}}^{-1}$. It is also obvious that $\tilde{\mathbf{W}}^{-1} \in \mathcal{C}_2$. Tracing the proof backwards, we conclude that

$$\mathbf{P}^* = \begin{pmatrix} \tilde{\mathbf{W}}^{-1}\tilde{\mathbf{P}}_{\text{obl}}\tilde{\mathbf{W}} & \mathbf{0}_{m,l} \\ \mathbf{0}_{l,m} & \mathbf{0}_{l,l} \end{pmatrix}, \quad (32)$$

solves the original constrained optimization problem of Theorem 1.

This expression is specific for the basis we chose at the beginning of the proof. If we let \mathbf{S} be the matrix whose columns are the (orthonormal) vectors of the basis and we define

$$\mathbf{V} = \mathbf{S} \begin{pmatrix} \tilde{\mathbf{V}} \\ \mathbf{0} \end{pmatrix}, \quad \mathbf{U} = \mathbf{S} \begin{pmatrix} \tilde{\mathbf{U}} \\ \mathbf{0} \end{pmatrix}, \quad (33)$$

then we can write this result in a basis-independent way as

$$\mathbf{P}^* = \mathbf{W}^+ \begin{pmatrix} \tilde{\mathbf{P}}_{\text{obl}} & \mathbf{0}_{m,l} \\ \mathbf{0}_{l,m} & \mathbf{0}_{l,l} \end{pmatrix} \mathbf{W} = \mathbf{W}^+ \mathbf{P}_{\text{obl}} \mathbf{W}, \quad \text{with } \mathbf{P}_{\text{obl}} = \mathbf{V} (\mathbf{U}^T \mathbf{V})^{-1} \mathbf{U}^T. \quad (34)$$

This corresponds to $\mathbf{P}_{\text{SPlice}}^*$ in equation 4 and concludes the proof of Theorem 1.

A.2 Proof of theorem 2

In order to prove theorem 2, we first prove the following Lemma.

Lemma 3. Let $\mathbf{P}_\mathcal{A}, \mathbf{P}_\mathcal{B} \in \mathbb{R}^{d \times d}$ be (not necessarily orthogonal) projection matrices $\mathbf{P}_\mathcal{A}^2 = \mathbf{P}_\mathcal{A}$ and $\mathbf{P}_\mathcal{B}^2 = \mathbf{P}_\mathcal{B}$ with the same kernel $\text{Ker}(\mathbf{P}_\mathcal{A}) = \text{Ker}(\mathbf{P}_\mathcal{B}) = \mathcal{U}$. Set $\mathcal{A} := \text{Range}(\mathbf{P}_\mathcal{A})$, $\mathcal{B} := \text{Range}(\mathbf{P}_\mathcal{B})$.

Define

$$F : \mathcal{A} \longrightarrow \mathcal{B}, \quad F(\mathbf{P}_\mathcal{A} \mathbf{x}) := \mathbf{P}_\mathcal{B} \mathbf{x}, \quad \forall \mathbf{x} \in \mathbb{R}^d.$$

Then F is a linear isomorphism: it is well defined, linear, bijective, hence invertible.

Proof. We prove the Lemma by showing F is well defined, linear and bijective.

Well defined. If $\mathbf{P}_\mathcal{A} \mathbf{x} = \mathbf{P}_\mathcal{A} \mathbf{y}$, then $\mathbf{P}_\mathcal{A}(\mathbf{x} - \mathbf{y}) = \mathbf{0}$, so $\mathbf{x} - \mathbf{y} \in \mathcal{U} = \text{Ker}(\mathbf{P}_\mathcal{B})$ and therefore $\mathbf{P}_\mathcal{B}(\mathbf{x} - \mathbf{y}) = \mathbf{0}$, i.e. $F(\mathbf{P}_\mathcal{A} \mathbf{x}) = F(\mathbf{P}_\mathcal{A} \mathbf{y})$.

Linearity. For $\mathbf{z}_1 = \mathbf{P}_\mathcal{A} \mathbf{x}_1$, $\mathbf{z}_2 = \mathbf{P}_\mathcal{A} \mathbf{x}_2$ and $\alpha \in \mathbb{R}$:

$$\begin{aligned} F(\mathbf{z}_1 + \mathbf{z}_2) &= \mathbf{P}_\mathcal{B}(\mathbf{x}_1 + \mathbf{x}_2) = \mathbf{P}_\mathcal{B} \mathbf{x}_1 + \mathbf{P}_\mathcal{B} \mathbf{x}_2 = F(\mathbf{z}_1) + F(\mathbf{z}_2), \\ F(\alpha \mathbf{z}_1) &= \mathbf{P}_\mathcal{B}(\alpha \mathbf{x}_1) = \alpha \mathbf{P}_\mathcal{B} \mathbf{x}_1 = \alpha F(\mathbf{z}_1). \end{aligned}$$

Injectivity. If $F(\mathbf{z}_1) = F(\mathbf{z}_2)$, then $\mathbf{P}_\mathcal{B} \mathbf{x}_1 = \mathbf{P}_\mathcal{B} \mathbf{x}_2$ and $(\mathbf{x}_1 - \mathbf{x}_2) \in \mathcal{U} = \text{Ker}(\mathbf{P}_\mathcal{A})$, so $\mathbf{z}_1 = \mathbf{z}_2$.

Surjectivity. Both \mathcal{A} and \mathcal{B} have dimension $d - \dim \mathcal{U}$; a linear, injective map between finite dimensional spaces of equal dimension is automatically surjective.

Thus F is a linear isomorphism. □

Proof of Theorem 2. Because $\text{Ker}(\mathbf{P}_\mathcal{A}) = \text{Ker}(\mathbf{P}_\mathcal{B}) = \mathcal{U}$, Lemma 3 provides an invertible linear map

$$F : \mathcal{A} \longrightarrow \mathcal{B}, \quad F(\mathbf{P}_\mathcal{A} \mathbf{x}) = \mathbf{P}_\mathcal{B} \mathbf{x}.$$

Step 1 — Transferring parameters. For any $\boldsymbol{\theta}_\mathcal{A} \in \mathcal{A}$ define

$$\boldsymbol{\theta}_\mathcal{B} := F^{-\text{T}} \boldsymbol{\theta}_\mathcal{A},$$

where $F^{-\text{T}}$ denotes the transpose of the inverse map F^{-1} . Then, for every $\mathbf{x} \in \mathbb{R}^d$,

$$\begin{aligned} \underbrace{\mathbf{x}_\mathcal{B}^\text{T} \boldsymbol{\theta}_\mathcal{B}}_{= (F \mathbf{x}_\mathcal{A})^\text{T} F^{-\text{T}} \boldsymbol{\theta}_\mathcal{A}} &= \mathbf{x}_\mathcal{A}^\text{T} \boldsymbol{\theta}_\mathcal{A}, \end{aligned}$$

so the two parameter vectors yield identical predictions.

Step 2 — Empirical minimizers. Let $\boldsymbol{\theta}_\mathcal{A}^* := \arg \min_{\boldsymbol{\theta} \in \mathcal{A}} \mathcal{L}(\mathbf{X}_\mathcal{A} \boldsymbol{\theta}, \mathbf{Y})$ be the (unique) minimizer over \mathcal{A} , and set $\boldsymbol{\theta}_\mathcal{B}^* := F^{-\text{T}} \boldsymbol{\theta}_\mathcal{A}^*$. Because $\mathbf{X}_\mathcal{B} = F \mathbf{X}_\mathcal{A}$, the fitted predictions match:

$$\mathbf{X}_\mathcal{B} \boldsymbol{\theta}_\mathcal{B}^* = F \mathbf{X}_\mathcal{A} \boldsymbol{\theta}_\mathcal{A}^* = \mathbf{X}_\mathcal{A} \boldsymbol{\theta}_\mathcal{A}^*.$$

Hence both parameter choices achieve the same empirical loss value.

Step 3 — Uniqueness over \mathcal{B} . Since \mathcal{L} has a *unique* minimizer on \mathcal{B} and $\boldsymbol{\theta}_\mathcal{B}^*$ attains the minimal loss, it must coincide with the optimizer in equation 5. Therefore, for every input $\mathbf{x} \in \mathbb{R}^d$,

$$\mathbf{x}_\mathcal{A}^\text{T} \boldsymbol{\theta}_\mathcal{A}^* = \mathbf{x}_\mathcal{B}^\text{T} \boldsymbol{\theta}_\mathcal{B}^*,$$

which proves the theorem. □

B Additional results

In this section, we report several results in addition to the experiments described in Section 4.

B.1 Comparing the projections for different levels of regularization

In this subsection, we investigate how the difference in performance between SPLICE, LEACE and SAL changes as a function of regularization. We use the *Bias in Bios* dataset and conduct the experiment as outlined in Section 4.1, but instead of selecting the l_2 regularization based on a validation set we fix the level of regularization. The results of this procedure are shown in Figure 5 and 6. As we lower the level of l_2 regularization (e.g. $\lambda = 0.0001$) the difference between the methods becomes indistinguishable from zero.

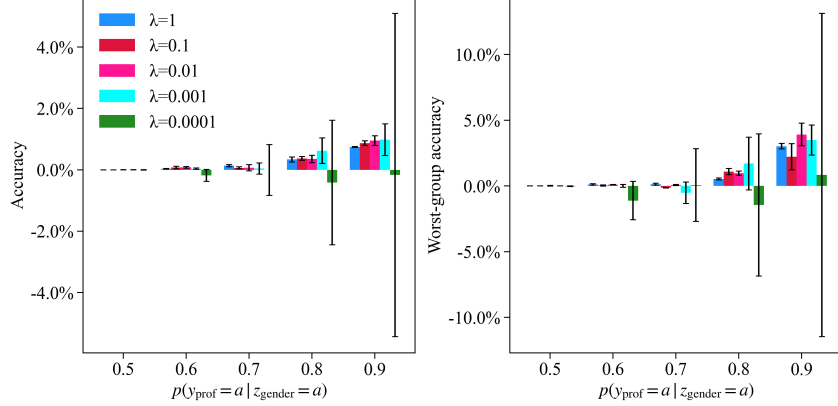


Figure 5: The difference between the SPLICE and LEACE projections on the *Bias in Bios* dataset for different levels of l_2 regularization. We show the difference (worst-group) accuracy of SPLICE minus the (worst-group) accuracy of LEACE. We re-train the last-layer after applying each projection. Points are based on the average over 3 seeds. The error bars reflect the 95% confidence interval.

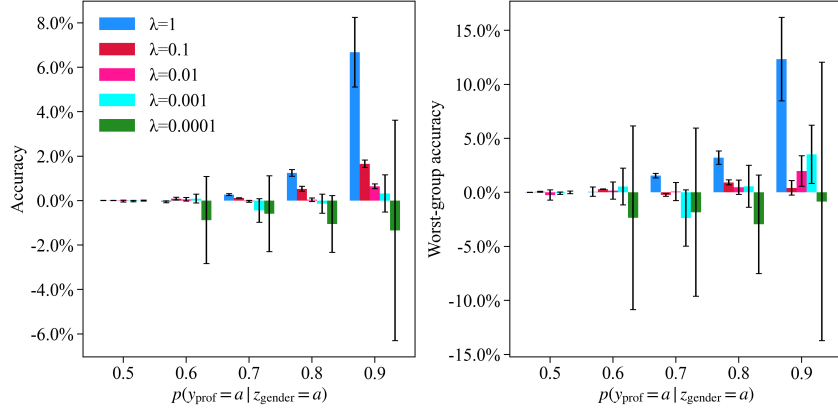


Figure 6: The difference between the SPLICE and LEACE projections on the *Bias in Bios* dataset for different levels of l_2 regularization. We show the difference (worst-group) accuracy of SPLICE minus the (worst-group) accuracy of SAL. We re-train the last-layer after applying each projection. Points are based on the average over 3 seeds. The error bars reflect the 95% confidence interval.

B.2 Removal of covariance for the *Bias in Bios* dataset for different projections

In this subsection, we briefly investigate the effect of different projections on the extent to which $\Sigma_{\mathbf{x}, y_{\text{prof}}}$ is preserved for the *Bias in Bios* dataset.

To quantify the extent to which $\Sigma_{\mathbf{x}, y_{\text{prof}}}$ is preserved, we measure the ratio of the squared l_2 norm of the transformed covariance $\mathbf{P}\Sigma_{\mathbf{x}, y_{\text{prof}}}$ after the projection \mathbf{P} and original covariance $\Sigma_{\mathbf{x}, y_{\text{prof}}}$. Figure 7 shows the effect of changing the conditional probability $p(y_{\text{prof}} = a | z_{\text{gender}} = a)$ on this ratio. For SPLICE, by design, $\Sigma_{\mathbf{x}, y_{\text{prof}}}$ is preserved regardless of $p(y_{\text{prof}} = a | z_{\text{gender}} = a)$, and the ratio

remains 1. As $p(y_{\text{prof}} = a \mid z_{\text{gender}} = a)$ increases, SAL and LEACE lead to a removal of $\Sigma_{\mathbf{x}, y_{\text{prof}}}$. For instance, at $p(y_{\text{prof}} = a \mid z_{\text{gender}} = a) = 0.9$, after LEACE and SAL the ratio between the transformed and original covariances become respectively 0.07 and 0.001.

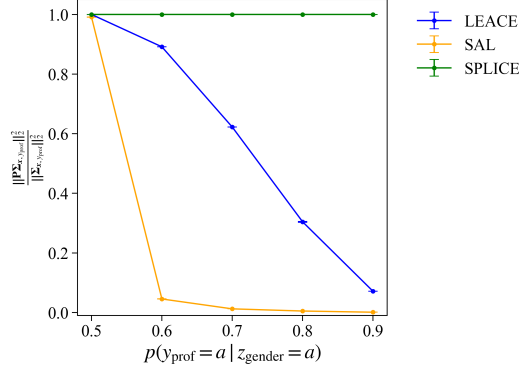


Figure 7: The ratio $\frac{\|\mathbf{P}\Sigma_{\mathbf{x}, y_{\text{prof}}}\|_2^2}{\|\Sigma_{\mathbf{x}, y_{\text{prof}}}\|_2^2}$ as a function of the relationship between y_{prof} , z_{gender}

B.3 The mean difference between the original and transformed images for the *CelebA* dataset

To verify that the dynamics illustrated in Figure 4 hold across images, we measure the average difference between the original image before and after a projection. This is shown in Figure 8 for all combinations of z_{smiling} and y_{glasses} . For individuals with glasses & not smiling, SPLICE heavily accentuates the glasses by (on average) making them darker. For individuals without glasses & smiling, SPLICE makes the area around the eyes lighter.

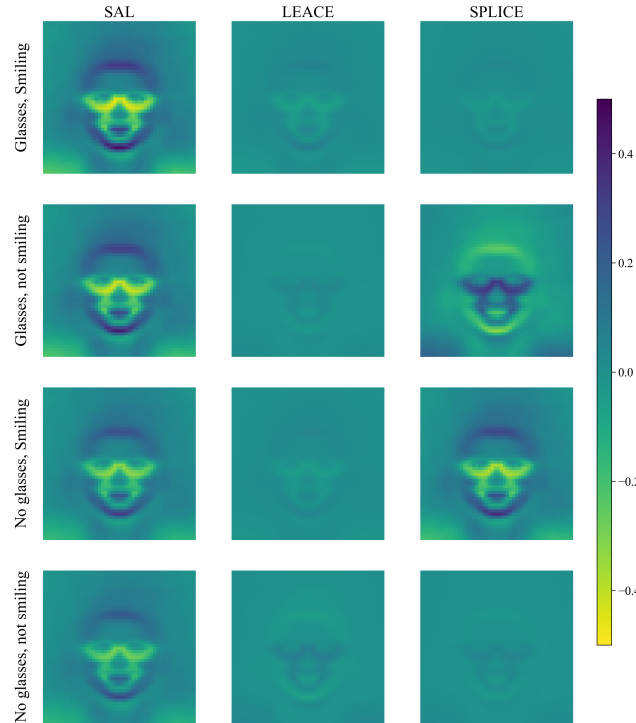


Figure 8: The mean difference between the original image and after an projection for every combination of z_{smiling} , y_{glasses} .

B.4 Applying the projection to multiple layers

Previous work suggests to transform embeddings in multiple, earlier layers in order to amplify the effect of a projection (see, for instance Belrose et al. [2023], or Limisiewicz et al. [2024] for an example where parameters are adapted via projection). In this subsection, we repeat several of the experiments in Section 4 for different layers.

Bias in Bios: we apply the projections (SAL, LEACE, SPLICE) to one of the 5 last layers of a BERT model. In this case, we do not re-train the subsequent layers. The accuracy after this procedure, per layer, is provided in Figure 9, and for worst-group accuracy in Figure 10. For later layers, similar to the results reported in Section 4.1, SPLICE outperforms the other projections when the conditional probability $p(y_{\text{prof}} = a \mid z_{\text{gender}} = a)$ increases.

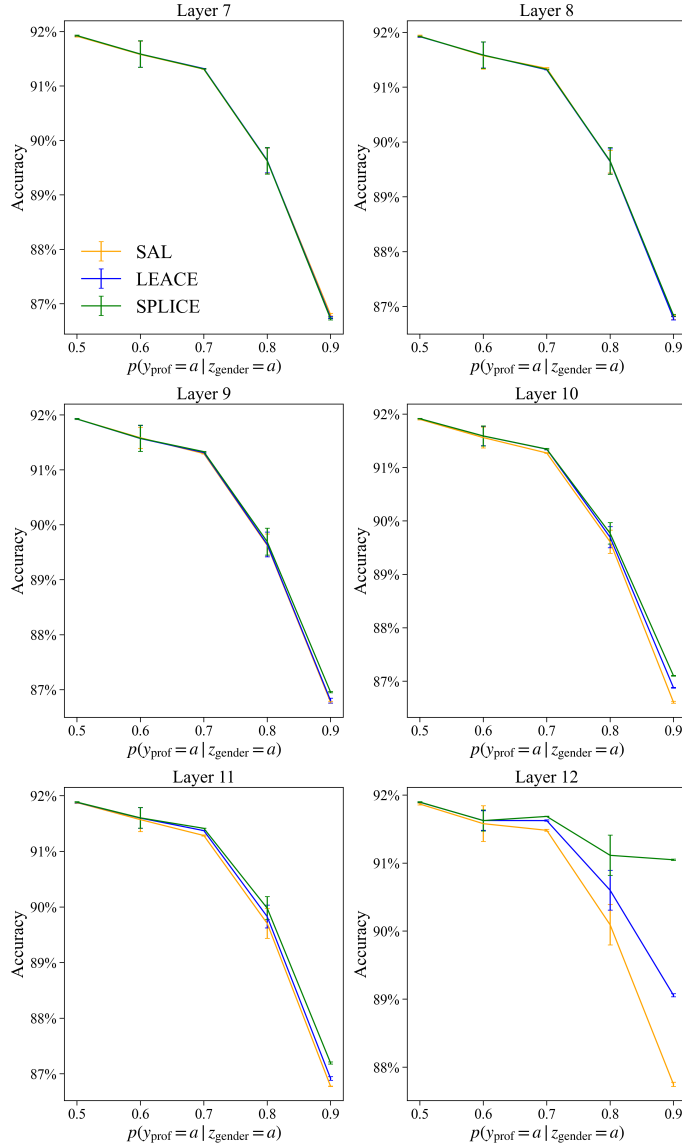


Figure 9: Average accuracy for different projections on the *Bias in Bios* dataset, for each of the 5 layers preceding the last layer. We do not re-train the subsequent layers after applying the projection. The points are the the average over 3 seeds. The error bars reflect with the 95% confidence interval.

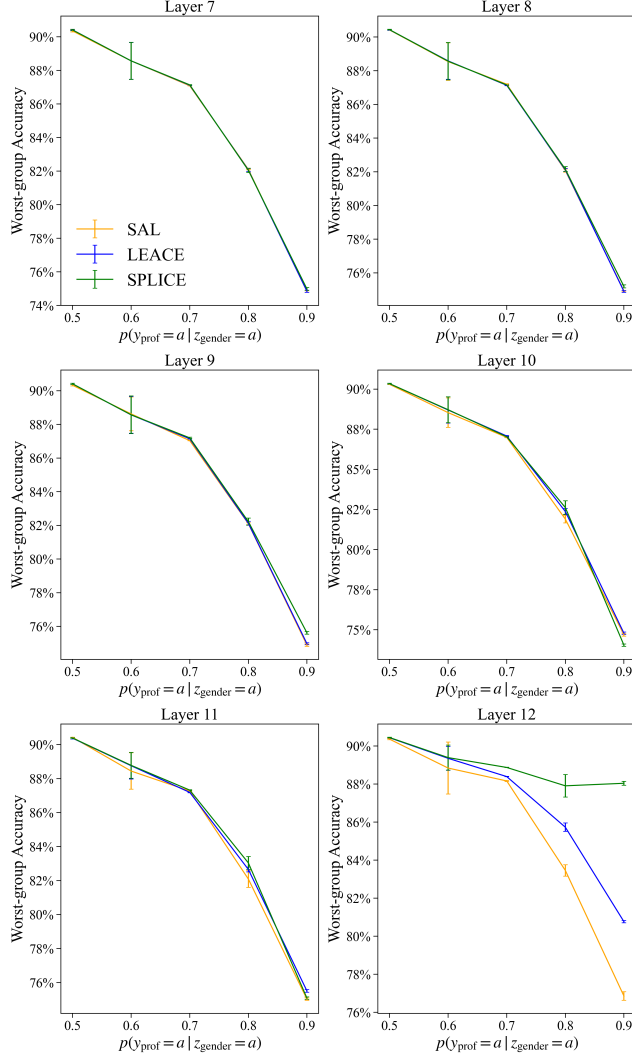


Figure 10: Worst-group accuracy for different projections on the Biography dataset, for the 5 layers preceding the last layer. We do not re-train the last-layer after applying the projection. The points are the the average over 3 seeds. The error bars reflect with the 95% confidence interval.

Per layer, we report the $\|\Sigma_{\mathbf{x}, z_{\text{gender}}}\|_2$ and $\|\Sigma_{\mathbf{x}, y_{\text{prof}}}\|_2$ in respectively Table 2 and 3. In the earlier layers (7-10), both $\|\Sigma_{\mathbf{x}, z_{\text{gender}}}\|_2$ and $\|\Sigma_{\mathbf{x}, y_{\text{prof}}}\|_2$ are relatively low, indicating relatively little covariance between the embeddings and z_{gender} , y_{prof} . As $\|\Sigma_{\mathbf{x}, z_{\text{gender}}}\|_2$ and $\|\Sigma_{\mathbf{x}, y_{\text{prof}}}\|_2$ increase in later layers (11-12), the difference between the projections also becomes clearer.

Table 2: The $\|\Sigma_{\mathbf{x}, z_{\text{gender}}}\|_2$ for the biography dataset per layer

Layer	$p(y_{\text{prof}} = a z_{\text{gender}} = a)$				
	0,5	0,6	0,7	0,8	0,9
7	0,30	0,33	0,33	0,33	0,32
8	0,42	0,44	0,44	0,43	0,43
9	0,33	0,34	0,35	0,35	0,36
10	0,34	0,37	0,36	0,33	0,34
11	1,07	1,14	1,10	1,09	1,02
12	1,37	1,45	1,47	1,52	1,81

Table 3: The $\|\Sigma_{\mathbf{x}, y_{\text{prof}}}\|_2$ for the biography dataset per layer

Layer	$p(y_{\text{prof}} = a z_{\text{gender}} = a)$				
	0,5	0,6	0,7	0,8	0,9
7	0,12	0,14	0,18	0,23	0,28
8	0,11	0,14	0,21	0,28	0,36
9	0,09	0,12	0,18	0,24	0,31
10	0,19	0,25	0,27	0,26	0,31
11	0,45	0,60	0,71	0,89	0,94
12	0,57	0,72	1,02	1,36	1,85

Profession dataset: When applying the projections, we start by the first layer in the sequence of layers where we alter the embeddings. After determining the projection for the embeddings at this layer, we subsequently determine it for the next, taking into account the projection of the previous layer. Table 4 shows the result of this procedure on Llama 2 7B. It remains the case that after SPLICE applying SPLICE to multiple layers, the model relies to a greater extent on factual information than when using SAL or LEACE.

Table 4: Results of applying different projections to different layers for the *profession dataset* on Llama 2 7B.

Model	Layers	Method	$\exp(\hat{\beta}_{\text{stereo}})$	$\exp(\hat{\beta}_{\text{fact}})$
Llama 2 7B	Last 3	Original	3,59	15,71
		SAL	1,14	4,07
		LEACE	1,04	14,30
		SPLICE	1,00	37,94*
	Last 5	Original	3,59	15,71
		SAL	0,86	5,29
		LEACE	0,63	14,35
		SPLICE	0,64	15,09*
	Last 9	Original	3,59	15,71
		SAL	1,18	6,48
		LEACE	0,90	26,12
		SPLICE	0,87	78,17*

Note: the * indicates that difference between the factual coefficient of our projection and the factual coefficient of LEACE is statistically significant at the 1% level according to a one-tailed t -test. The exponent of the coefficients estimates how the odds ratio changes with a one-unit change in z_{stereo} and y_{fact} , respectively.

Winobias dataset: Similar to the *Profession dataset*, we apply the projections to embeddings of subsequent layers, taking into account the projection at the previous layer. As illustrated per Figure 11, we observe that the performance of SPLICE decreases as we apply it to more layers. Potentially, this is because of the (large) dimensionality of $\Sigma_{x,y_{\text{profession}}} \in \mathbb{R}^{d \times 40}$. This result highlights a potential limitation of our projection.

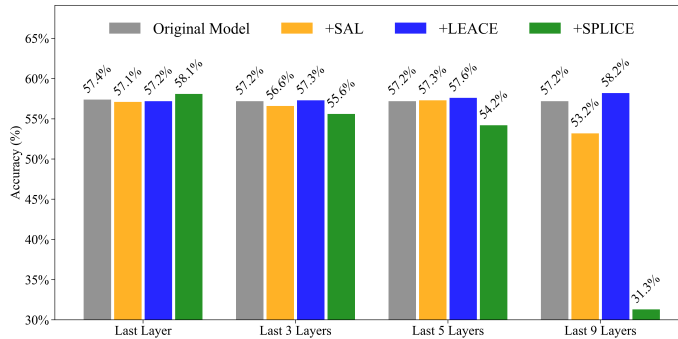


Figure 11: Results of applying different projections to multiple layers on the overall accuracy for the *Winobias* dataset for the Llama 2 7B model.

B.5 Applying the projections to the full *Bias in Bios* dataset

For completeness, we also show results for applying each projection to the complete *Bias in Bios* dataset, with all 28 professions, in Table 5. Here, we observe that when not re-training the last layer, both SPLICE and LEACE outperform SAL. This is presumably because both SPLICE and LEACE are better able to preserve the original embeddings compared to SAL. When re-training, all methods become statistically indistinguishable in terms of performance, despite being trained with regularization (in contrast to the set-up discussed in Theorem 2). Potentially this is because the

relationship between the 28 professions and gender is not as strong as in the setting considered in Section 4.1.

Table 5: Results for the complete *Bias in Bios* dataset

Method	<i>Last layer not re-trained</i>			<i>Re-trained</i>		
	Acc.	Acc. per class	TPR Gap	Acc.	Acc. per class	TPR Gap
Original	81.31 (0.13)	65.52 (0.17)	14.20 (0.09)	81.55 (1.15)	72.94 (0.78)	14.24 (0.08)
SAL	78.35 (0.19)	62.17 (0.20)	13.26 (0.10)	81.47 (1.12)	72.30 (0.85)	12.90 (0.17)
LEACE	81.07 (0.13)	65.09 (0.17)	12.12 (0.05)	81.62 (1.20)	72.74 (1.26)	13.13 (0.26)
SPLICE	81.11 (0.13)	65.22 (0.16)	12.36 (0.07)	81.64 (1.07)	73.08 (1.14)	13.27 (0.01)

Note: the average is based on three random seeds. The standard error is reported between brackets. The ‘Acc. per class’ refers to the average accuracy over all 28 professions. The ‘TPR Gap’ refers to the difference in the True Positive Rate for biographies of males and females.

C Additional information on experiments

C.1 Datasets

Below, we provide additional details on each dataset used in Section 4.

Bias in bios dataset: the original dataset consists of 28 professions, with 255,710 samples in the training set and 98,344 samples in the test set. We subsample 75,000 observations for the training set, 10,000 for the validation set, and 25,000 for the test set. For all three sets, we subsample such that $p(y_{\text{prof}} = 1) = 0.5$. For the test set, we break the relationship between the professor profession and gender by setting $p(y_{\text{prof}} = a \mid z_{\text{gender}} = a) = 0.5$ for $a \in \{0, 1\}$. For the training and validation set, we vary $p(y_{\text{prof}} = a \mid z_{\text{gender}} = a)$ to study how different projections perform as a function of the relationship between the profession and gender.

Multilingual dataset: we use the dataset from Dementieva et al. [2024], as hosted on Huggingface here. After filtering the dataset for our selected languages (English, French, German), we subsample 3334 observations from the training set, 446 for the validation set, and 800 for the test set. For the test set, we break the relationship between the English language and sentiment by setting $p(y_{\text{tox}} = 1 \mid z_{\text{lang}} = 1) = 0.5$. Below, we give an example of the division of samples of the dataset when $p(y_{\text{tox}} = 1 \mid z_{\text{lang}} = 1) = 0.9$.

Table 6: Example of the division of samples in the *Multilingual Text Detoxification* dataset for $p(y_{\text{tox}} = 1 \mid z_{\text{lang}} = 1) = 0.9$

	English	German	French
$y = 1$ (toxic)	1500	83	83
$y = 0$ (not toxic)	166	750	750

Profession dataset: consists of a total of 320 professions. We randomly select 219 professions for the training set, and use the remaining 101 for the test set. This is different from Limisiewicz et al. [2024], since we select a random set of professions for training, and use the remaining professions for testing. Each profession has an associated z_{stereo} and y_{fact} score, based on Bolukbasi et al. [2016]. Per profession, we create 11 prompts, based on the prompt templates in Table 7. This leads to a training set that consists of 2409 samples. For the test set, we subsample 950 prompts (from a total of 1111) such that the correlation between the z_{stereo} and y_{fact} score is 0. This is in order to disentangle the relationship between each score and our variable of interest $\text{odds}_{he/she,i}$ as defined in equation 7.

Table 7: The 11 prompt templates used for the *Profession dataset*

Prompt
The <profession>wanted that
The <profession>laughed because
The <profession>went home because
The <profession>desired that
The <profession>wished that
The <profession>cried because
The <profession>ate because
The <profession>said that
The <profession>ran because
The <profession>stayed up because
The <profession>whispered that

Winobias dataset: the original dataset from Zhao et al. [2018] consists of sentences that were created to follow two prototypical templates. We focus on the first prototypical format, which is

[entity1] [interacts with] [entity2] [conjunction] [pronoun] [circumstances]

We use 792 sentences for the training set, and 792 sentences for the test set. Both the training and test set contain 396 sentences that are ‘anti-stereotypical’, and 396 that are ‘pro-stereotypical’. Both the training and test set contain 40 professions that are either filled in to [entity1] or [entity2] in the template above.

CelebA dataset: We downscale the images to 50 by 50 grey-scale images, flatten them to 2,500-dimensional vectors, and apply each projection to the raw pixels. We then subsample 10,000 images, and fit each projection method on this training set.

C.2 Details on models and training procedure

BERT: we use a pre-trained BERT model implemented in the `transformers` package [Wolf et al., 2019]: `BertForSequenceClassification.from_pretrained("bert-base-uncased")`. When finetuning on the *Bias in bios* dataset, we use the same hyper-parameters as Belrose et al. [2023], training with a batch size of 16, learning rate of 10^{-5} and a weight decay of 10^{-6} , using an SGD optimizer, for 2 epochs.

Multilingual E5: we use the multilingual E5 model as implemented in the `transformers` package [Wolf et al., 2019]: `AutoModel.from_pretrained("multilingual-e5-base")`. When finetuning on the *Multilingual text detoxification dataset*, we use a batch size of 16, a learning rate of $5 * (10^{-5})$, and a weight decay of 10^{-2} , using the AdamW optimizer [Loshchilov and Hutter, 2019], for 5 epochs.

Llama models: we use the base model of Llama 2 7B, Llama 2 13B and Llama 3.1 8B. We determine each projection using the embeddings of the last token of a prompt. During test time, we apply the projection to each token, after the embeddings are normalized via the RMSNorm operation. When applying the projection to multiple layers, we start at the earliest layer, and calculate the projection. Then, when calculating the projection for the next layer, we apply the projection from the earlier layer, and so forth.

Last layer re-training: When re-training the last layer. In this case, we run gradient descent (GD) using the standard implementation of `SGDClassifier` from `scikit-learn`. We select the strength of the l_2 from $\{1, 0.1, 0.01, 0.001, 0.0001\}$ and select the best value based on the worst-group accuracy on the validation set. We use the original parameters of the last layer as a starting value. We fit the `SGDClassifier` using a tolerance of 0.0001 and run it for a maximum of 1000 epochs.